FIBER COMPOSITE ELEMENTS AND TECHNIQUES AS NON-METALLIC REINFORCEMENT OF CONCRETE

BRITE PROJECT 4142 / BREU - CT 91 0515

Evaluation of potentials and production technologies of FRP
Technical report Task 1

F.S. Rostásy, Editor

Report No.: BREU 1-92

SICOM AKZO HBG iBMB/TU Braunschweig Magnel Laboratory Gent

September 1992

TABLE OF CONTENTS

SUB-TASK 1.2 REVIEW AND APPRAISAL OF THE PROPERTIES OF UD-FRP ELEMENTS AND THEIR PRODUCTION TECHNOLOGIES

NOTATIONS

(in accordance to EC2. pt.1)

1. UNITS

For calculations, the following units are recommended:

- forces and loads : kN, kN/m, kN/m^2
- unit mass : kg/m^3
- unit weight : kN/m^3
- stresses and strengths : N/mm^2 (= MPa; = MN/m^2)
- moments (bending...) : kNm
- strain : °/∘∘

2. LATIN UPPER CASE SYMBOLS

2.1 Geometry

A	Area (in general)
A_b	Total cross sectional area of a concrete section
$A_{b,eff}$	Effective tensile zone of reinforcement
A_{bt}	Tensile zone in the uncracked state of concrete
A_c	Total cross sectional area of a composite element
A_f	Total cross sectional area of fibers
A_m	Total cross sectional area of resin matrix
A_p	Area of a prestressing steel unit
A_s	Area of reinforcement within the tensile zone
$A_{s,min}$	Minimum area of longitudinal tensile reinforcement
A_{s1}	Area of tension reinforcement effective at the section
A_{s2}	Area of compressive reinforcement
$A_{s,prov}$	Area of steel provided
$A_{s,req}$	Area of steel required
$A_{s,surf}$	Area of surface reinforcement
A_{st}	Area of a transverse bar
A_{sv}	Additional transverse steel perpendicular to the lower face
I_b	Second moment of area of a concrete section
R	Curvature radius of tendon
T	Torsional moment
W_b	Section modulus of concrete
W_t	Torsional resistance moment

2.2 Actions, Resistances, Forces and Moments

A	Accidental action
G	Permanent action
P	Prestressing force
Q	Variable action
S	Characteristic action
S_d	Design action
R	Resistance
R_d	Design resistance
R_k	Characteristic resistance
F	Force (in general)
F_c	Short-term tensile force of total composite cross-section
F_f	Short-term tensile force of total fiber cross-section
F_p	Short-term tensile force of prestressing steel
F_s	Short-term tensile force of reinforcing steel
F_{ck}	Characteristic short-term tensile breaking force of the composite
F_{fk}	Characteristic short-term tensile breaking force of total fiber cross-section
F_{pk}	Characteristic short-term breaking force of prestressing steel unit
F_{sk}	Characteristic short-term tensile breaking force of reinforcing steel
F_{cl}	Long-term force of total composite cross-section
F_{fl}	Long-term tensile breaking force of total fiber cross-section
F_{clk}	Characteristic long-term static breaking force of the composite element
F_{flk}	Characteristic long-term tensile force of total fiber cross-section
F_{cli}	Long-term force on force level a_i
F_{cm}	Mean short-term tensile breaking force of the investigated lot of FRP-elements
F_{cr}	Failure load after long-term loading of the composite
M	Bending moment (in general)
M_{cr}	Moment causing cracking
M_{Sd}	Design value of the applied internal bending moment
M_u	Ultimate bending moment
N_{Sd}	Design axial force (tension or compression)
N_u; N_{ud}	Design ultimate capacity of the section subjected to axial load only

P_d Design value of the prestressing force at the ultimate limit state

$P_{k,inf}$; $P_{k,sup}$ Lower and upper characteristic value of the prestressing force for serviceability calculations

P_o Initial force at the active end of the tendon immediately after stressing

$P_{o,max}$ Maximum permissible value of P_o

$P_{m,o}$ Mean value of the prestressing force immediately after stressing (post-tensioning) or transfer (pre-tensioning) at any point distance along the member (i.e. the force after immediate losses have occured)

$P_{m,t}$ Mean value of the prestressing force at time t, at any point distance x along the member

$P_{m,\infty}$ Mean value of the prestressing force, after all losses have occured, at any point distance x along the member

V_u Ultimate shear capacity

DP Loss of prestress

DP_c Loss of prestress due to elastic deformation of the member at transfer

DP_{sl} Loss of prestress due the anchorage slip

$DP_{\mu}(x)$ Loss of prestress due to friction

$DP_c(t)$ Loss of prestress due to creep, shrinkage and relaxation at time t

2.3 Materials

E_b Modulus of elasticity of normal weight concrete

E_{bd} Design value of the secant modulus of elasticity

E_{bm} Secant modulus of elasticity of normal weight concrete

$E_b(t)$ Tangent modulus of elasticity of normal weight concrete at time t

$E_{b(28)}$ Tangent modulus of elasticity of normal weight concrete at 28 days

$E_{bc,eff}$ Effective modulus of elasticity of normal weight concrete

E_{Lc}; $E_{Lb,m}$ Secant modulus of elasticity of lightweight concrete

E_c Modulus of elasticity of composite

E_f Modulus of elasticity of fiber

E_m Modulus of elasticity of matrix

E_s Modulus of elasticity of reinforcement or prestressing steel

3. LATIN LOWER CASE LETTERS

3.1 Geometry

b	Overall width of a cross-section, or actual flange width in a T or L beam
b_{eff}	Effective flange width of a T or L beam
b_z	Width of the tensile cross section
b_w	Width of the web on t, I or L beams
$b_{w,nom}$	Effective width of the web
c	Concrete cover
min c	Minimum concrete cover
d	Effective depth of a cross-section
$\ddot{A}_n$	Diameter of a prestressing duct
d_g	Largest nominal maximum aggregate size
d_c	Diameter of a composite bar,etc.
d_f	Diameter of an individual fiber
d_s	Diameter of a reinforcing or prestressing bar
e	Eccentricity
f	Deflection
$f_{c,s}$	Increase of deflection due to creep and shrinkage
f_{tot}	Total deflection
h	Overall depth of a cross-section
h_f	Overall depth of a flange in T or L beams
k	Unintentional angular displacement of the tendons
l	Length, span (in general)
l_b	Basic anchorage length for reinforcement
l_{ba}	Anchorage length over which the tendon force in pretensioned members is fully transmitted to the concrete
l_{bp}	Transmission lenghth over which the prestressing force is fully transmitted to the concrete
l_c	Free length between anchorages
l_e	Gage length for the measurement of the axial strain
l_{eff}	Effective span of a beam
l_n	Clear distance between the faces of the supports
l_o	Length of span(s) between points of zero moment
$l_{p,eff}$	Dispersion length, over which the concrete stresses gradually disperse to a linear distribution across the section (effective transfer)
s	Spacing of the stirrups
s_v, s_h	Minimal vertical or horizonal distance of tendons

u	Perimeter of concrete cross section, having area A_b
v_f	Fiber volume in a composite cross section
v_m	Matrix volume in a composite cross section
w_k	Design crack width
x, y, z	Coordinates
z	Lever arm of internal forces
z_{cp}	Distance between the centre of gavity of the concrete section and the tendons

3.2 Materials

f	strength (in general)
f_b	Compressive strength of concrete
$f_{bk,cube}$	Characteristic compressive cube strength of concrete at 28 days
f_{bm}	Mean value of concrete cylinder compressive strength
f_{btk}	Characteristic axial tensile strength of concrete
f_{btm}	Mean value of axial tensile strength of concrete
$f_{btk,0.05}$	Lower characteristic tensile strenth (5% fractile)
$f_{btk,0.95}$	Upper characteristic tensile strength (95% fractile)
$f_{bt,ax}$	Axial tensile strength of concrete
$f_{bt,fl}$	Flexural tensile strength of concrete
$f_{bt,sp}$	Splitting tensile strength of concrete
f_c	Tensile strength of composite
f_{ck}	Characteristic tensile strength of composite
$f_{c\tau i}$	interlaminar shear strength of a composite
$f_{c\tau s}$	surface strength of a composite
f_τ	bond strength between composite and concrete
f_f	Tensile strength of fiber of a composite
f_{fk}	Characteristic short-term tensile strength of fiber
f_m	Tensile strength of matrix of a composite
f_{mk}	Characteristic strength of matrix of a composite
f_p	Tensile strength of prestressing steel
f_{pk}	Characteristic tensile strength of prestressing steel
$f_{p0.1}$	0.1% proof-stress of prestressing steel
$f_{p0.1k}$	Characteristic 0.1% proof-stress of prestressing steel
f_t	Tensile strength of reinforcement
f_{tk}	Characteristic tensile strength of reinforcement
f_y	Yield stress of reinforcement

f_{yd}	Design yield strength of reinforcement
f_{yk}	Characteristic yield stress of reinforcement
f_{ywd}	Design yield strength of stirrups

4. GREEK LOWER CASE LETTERS

4.1 Geometry

a	Inclination of shear reinforcement to the member axis
a	Angle, ratio
b	Spread angle of the prestressing force
l	Ratio (A_s/A_b)
l	Coefficient of friction between the tendons and their ducts

4.2 Strain and Stress

a_i	Force level (F_{cli}/F_{cm})
e	Strain (in general)
e_u	Ultimate strain
e_b	Compressive strain in the concrete
e_{bu}	Ultimate compressive strain in the concrete
e_{bs}	Basic shrinkage strain for normal weight concrete
$e_{bs\infty}$	Final shrinkage strain for normal weight concrete
e_u	Elongation of reinforcement or prestressing steel at maximum load
e_c	Elongation of composite at maximum load
e_{cc}	Creep strain
ϵ_f	Elongation of fiber at maximum load
e_m	Elongation of matrix at maximum load
e_p	Elongation of prestressing steel at maximum load
e_t	Elongation of reinforcing steel at maximum load
De_c	Variation of elongation in the composite
De_p	Variation of elongation in the prestressing steel
r	Stress (in general)
$r(t_0);r(t)$	Stress at time t_0 or t
r_b	Stress in concrete
r_{bg}	Stress in the concrete adjacent to the tendons, due to self-weight and any other permanent actions
r_{bp0}	Initial stress in the concrete adjacent to the tendons, due to prestress

r_{bS}	Compressive stress in the centre of gravity of a concrete cross section
r_{bt}	Tensile stress in concrete
r_c	Stress in a fiber composite
r_f	Stress in an individual fiber of a composite
r_m	Stress in matrix
r_p	Stress in prestressing steel
r_m; r_u; r_o	Middle-, lower- and upper stress under dynamic action
Dr_{pr}	Variation of stress in the tendons at section x due to relaxation
$Dr_{p,c+s+r}$	Variation of stress in the tendons due to creep, shrinkage and relaxation
s	Shear stress
Dr	Stress variation between lower and upper stress
Dr_{rel}	Variation of stress of a composite due to relaxation

4.3 Material

a	Ratio (E_s/E_b or E_c/E_b)
a	Coefficient of linear thermal expansion (in general)
$a_{T,b}$	Coefficient of linear thermal expansion of concrete
$a_{T,c}$	Coefficient of linear thermal expansion of a fiber composite
$a_{T,s}$	Coefficient of linear thermal expansion of reinforcing or prestressing steel
a_{cl}	Coefficient of linear thermal expansion of composite (longitudinal)
a_{ct}	Coefficient of linear thermal expansion of composite (transversal)
a_{fl}	Coefficient of linear thermal expansion of fiber (longitudinal)
a_{ft}	Coefficient of linear thermal expansion of fiber (transversal)
a_m	Coefficient of linear thermal expansion of matrix
q	Density
q_b	Density of concrete
q_c	Density of the composite element
q_f	Density of fibers
q_m	Density of matrix
l_b	Poisson's ratio of concrete
l_c	Poisson's ratio of composite
u	Creep function
w	Relaxation function

4.4 Safety

c_A	Partical safety factors for accidental actions A
c_B	Partial safety factors for concrete material properties
c_F	Partial safety factors for actions, F
c_G	Partial safety factors for permanent actions G
c_M	Partial safety factor for material property, taking account of uncertainties in the material properties itself and in the design model used
c_P	Partial safety factors for actions associated with prestressing, P
c_Q	Partial safety factors for variable actions Q
c_S	Partial safety factor for the properties of reinforcement and prestressing steel
c_f	Partial safety factor for actions without taking account of model uncertainties
c_g	Partial safety factor for permanent actions without taking account of model undertainties
c_m	Partial safety factor for a material property, taking account only of uncertainties in the material property

5. OTHER SYMBOLS

N	Number of load cycles
N_u	Number of load cycles until fracture
T	Temperature
DT	Temperature difference
n	Total number of wires and strands in a tendon
t	Time being considered
t_0	Time at initial loading of concrete
t_u	Time under load until fracture
t_{ui}	Time under force F_{cli} until fracture
l	Mean value
r	Standard deviation
v	Coefficient of variation

SUB-TASK 1.1 REQUIREMENTS FOR FRP FOR CONCRETE APPLICATION

1. PRINCIPAL OBJECTIVES

Sub-task 1.1 of the work program of BREU-91 05 15 deals with the formulation of the main requirements high-strength FRP tensile elements will have to meet in order to be economically and successfully applied for reinforced and prestressed concrete construction. These requirements must be studied and formulated with respect to the following criteria:

a) Service of performance of structural concrete members, deformation, cracking, stiffness under service load and environmental influence.

b) Load carrying capacity when loaded in bending, by normal forces and in shear etc.

c) Design of structural concrete members by taking into account the specific properties of FRP and by considering the optimal technical and economic utilization of the virtues of FRP.

d) Aspects of the production of precast concrete members and of on-site works taking into account the specific properties of FRP.

These aspects will be dealt with further-on on basis of our knowledge on structural concrete reinforced or prestressed with steel.

2. ON DEVELOPMENT AND INITIAL APPLICATIONS OF FRP TENSILE ELEMENTS

Structural concrete members are conventionally reinforced and/or prestressed by steel elements, in the shape of bars and meshes and/or prestressing steel elements such as wires, bars or strands. In structural concrete, the steel is embedded in concrete or cementitious grout and thereby protected against corrosion by the high alkalinity of the pore solution of the concrete cover or of the grout as long as the passivity of the steel surface exists. In spite of this undisputable protective property of concrete and grout, premature losses of durability due to steel corrosion are being increasingly observed all over the world. This is especially true if the structural members are subjected to severe environmental exposure. Serious technical and economic damages arise, endangering the structural integrity, shortening the span of service life of structures.

Structural concrete industry has reacted to these damages in many ways. A plurability of structural, technological and executional countermeasures were developed to enhance durability. Roughly speaking, two main avenues of development can be distinguished. One avenue adheres to steel as reinforcing and prestressing material but exploits all possibilities for an improved active and passive protection of the steel against corrosion (e.g. low-permeability concrete, zinc and epoxy coating of steel, etc.). The other avenue represents the quest for new non-corroding materials as an alternative to steel. Because stainless steel is unacceptable for structural concrete due to its cost this quest inevitably led to Fiber Reinforced Plastics, abbreviated FRP.

FRP are a group of advanced composite materials. FRP are not an invention but the result of steady evolution. They are not in a static but already in a dynamic state of development. This evolution was initiated by a variety of industries for engineering applications other than structural concrete. Today, FRP are indispensable materials for aircrafts, automobiles, for many types of sports gear etc. The structural concrete industry is the beneficiary of this evolution.

There are many types of FRP, with more to emerge in the future. FRP consist of thin and strong fibers of different chemical origin embedded in a matrix. Because here the potential use of FRP as high-strength tensile elements for structural concrete is in the focus of attention, only the unidirectional (ud) arrangement of virtually endless fibers in a polymeric resin matrix will be dealt with. It should be mentioned that for the above-mentioned other applications the multidirectional (md) arrangement of fibers is predominantly used to obtain plate-shaped elements (laminates). It is expected that in future the use of md-laminates for structural profiles will gain momentum. Such profiles will lead to solutions competetive to structural steel.

The FRP tensile elements - in the shape of rods, strips, strands, and also in thin plates - which are suitable for the reinforcing and/or prestressing of concrete members, exhibit a series of assets. Some of these assets make FRP equivalent to reinforcing or prestressing steel, others prove to be superior. These assets comprise:

- high and adjustable tensile strength and modulus of elasticity,
- excellent corrosion resistance to a plurality of environments aggressive to steel,
- very low specific weight,
- magnetic and electric neutrality.

It should not be suppressed that there are also drawbacks. One serious obstacle is the high price of FRP per weight unit at present. But as FRP are being increasingly used for many applications mainly other than civil engineering structures, their price decreases from year to year. Besides if the price per tonne of force is considered the economic gap between prestressing steel and FRP is rapidly vanishing, with FRP weighing one sixth to one fourth of steel per volume.

FRP are strong when stressed axially but very sensitive against lateral pressure. This phenomenon calls for new ways of anchorage design and of structural detailing. Some types of FRP are sensitive to the high alkalinity of concrete, others however are entirely insensitive.

The above described assets of FRP caught the interest of the structural concrete industry searching for a non-corroding alternative to steel. In cooperation with the chemical industry and scientists all over the world FRP high-strength tensile elements are being developed and applied. Strong activities of technical committee work can be observed. International conferences report on the state of art which is in steady progress.

Following laboratory research, first applications in real scale are realized in many countries. Especially in Europe and Japan, first bridges and structures using FRP tensile elements for the pre- and post-tensioning of concrete are being built. Some of these applications have already been in service successfully for five to ten years. FRP are also being used for the epoxy-bonded external strengthening of concrete structures.

FRP are a materials group in many ways different from reinforcing and prestressing steel. This calls for new ways of testing and design, of structural detailing and for new methods for the reliable anchorage and transfer of force. To give guidance in these problems is the goal of this report.

3. METHOD OF VALIDATION OF THE PROPERTIES OF FRP ELEMENTS

If in the future FRP should be increasingly used as a non-corroding alternative to prestressing and reinforcing steel for structural concrete applications a comparison of the most important properties with steel can serve as a starting point for the validation of FRP.

Reinforcing and prestressing steels are well-developed materials. They are standardized in most countries. The requirements and values shown in Table 3.1 represent a compilation of properties mainly on basis of the European Standards pr EN 10198 and pr EN 10080. The main purpose of this table is to serve as a checklist of properties to be known or discussed or to be used for reference.

In Table 3.2 the properties of reinforcing steel and prestressing steel are compared with the properties of the fiber of the equivalent FRP tensile elements as they are developed and known until now.

A fundamental difference between steel and the FRP elements is steel being a one component material and FRP consisting of at least two components. FRP is therefore also called a composite. A FRP element can be modified either by changing the properties of the fiber or the matrix or by changing both. A further difference which has to be taken into account is the fact that steel is more or less an isotropic material and FRP an anisotropic one. The properties in different directions can therefore differ dramatically in FRP tensile elements. The findings on material properties of SUB-TASK 1.2 are taken into account.

Table 3.1: Requirements for Reinforcing and Prestressing Steel

Properties		unit	STEEL reinforcing	STEEL prestressing
COMPOSITION		•	a.p.	a.p.
MANUFACTURING		•	a.p.	a.p.
GEOMETRY				
SHAPE (W=wire,R=rod,I=strip,A=strand)		•	W,R	W,R,A
diameter		mm	4 to 40	4 to 8
profile		•	a.p.	a.p.
straightness (arrow of a 1 m bow)		mm	no straightenin	<25
MECHANICAL				
linear strength	- short time	MPa	340 to 550	500 to 2000
	- after 100 years	MPa	•	•
radial strength (% of linear strength)		%	•	•
E-modulus	- axial	GPa	•	•
	- radial	GPa	•	•
strain	- rupture	%	>2,75 to 5	>3,5
	- purely elastic	%		
deformation capacity		?		
Poisson ratio		•	•	•
suitability for bending		•	1	>3 to 4
0,1% strainforce		kN	•	18,5 to 69,7
0,2% strainstress		MPa	220 to 500	•
constriction		%	•	<25
CONDITION OF THE SURFACE		•	a.p.	a.p.
MISCELLANEOUS				
relaxation/creep after 1000 hours at "using stress"		%	•	1,5-4
fatigue		•	no failure	no failure
stress rupture (in an ammonium rhodanide environment)		h	•	1,5
transfer length (dependent of Poisson ratio and profile)		mm	•	•
thermal expansion coefficient	- axial	10E-6/°C	•	•
	- radial	10E-6/°C	•	•
thermal resistance (temperature at 90% of strength)		°C	•	•
fire resistance		•	•	•
corrosivity in:	- neutral concrete	•	•	•
	- chloride concrete	•	•	•
	- alkaline concrete	•	•	•
electrical conductivity		•	•	•
EXECUTION ASPECTS (irrelevant for bare fibres)				
weight		g/cm3	•	•
flexibility		•	•	•
anchoring		•	•	•
vulnerability with transport/storage/execution		•	•	•

a.p. as prescribed • no requirement

Table 3.2: Properties of FRP-Elements in Comparison with Steel

		STEEL		ARAMID		CARBON		GLAS	
Properties	unit	reinforcing	prestressing	fibre	composite*	fibre	composite*	fibre	composite*
COMPOSITON	•	•	•	•	•	•	•	•	•
MANUFACTURING	•	•	•	•	•	•	•	•	•
GEOMETRY									
SHAPE (W = wire, R = rod, I = strip, A = strand)	•	W,R	W,R,A	•	R,I	•	R,A	•	R,A
diameter	mm	4 to 40	4 to 8	20 to 400 kfil	2,5 to 7,5	•	?	•	2 to 20
profile	•	0	0	•	+ +	•	+	•	+
straightness (arrow of a 1m bow)	mm	•	< 25'	•	?	•	?	•	?
MECHANICAL									
linear strength – short time	MPa	340 to 650	1000 to 2000	3000	increase	3400	no change?	2300	no change?
– after 100 years	MPa	•	1000 to 2000	±2700	increase	±3150	no change?	?	no change?
radial strength (% of linear strength)	%	100	100	•	< 10	•	10 to 100	•	10 to 100
E-modulus (') – axial	GPa	205	205	125	–	240	–	70	–
– radial	GPa	205	205	±5'	–	10'	–	70	–
strain – rupture	%	6 to 15	4	2,3	slight increase	1,4	?	3,2	?
– purely elastic	%	?	?	?	?	?	?	?	?
deformation capacity	?	?	?	?	?	?	?	?	?
Poisson ratio	•	0,3	0,3	?	0,38	?	?	?	?
suitability for bending	•	•	•	•	?	•	?	•	?
0,1% strainforce	kN	•	•	?	increase	?	no change?	?	no change?
0,2% strainstress	MPa	•	•	?	increase	?	no change?	?	no change?
constriction	%	•	•	•	•	•	•	•	•
CONDITION OF THE SURFACE	•	•	•	•	•	•	•	•	•
MISCELLANEOUS									
relaxation/creep after 1000 hours at "using stress"	%	•	5 to 15	25	no change?	?	?	5	?
fatigue	•	•	•	+ +	no change?	+ +	?	– – to –	?
stress rupture (in an ammonium rhodanide environment)	h	?	?	•	•	•	•	•	•
transfer length (dependent of Poisson ratio and profile)	mm	400' to 600'	400' to 600'	•	50 to 1000'	200' to 400'		200' to 400'	
thermal expansion coefficient – axial	10E-6/°C	12	12	-3,4	-2	-0,1 to -1,5	?	4 to 5	?
– radial	10E-6/°C	12	12	60	80	10 to 30	?	4 to 5	?
thermal resistance (temperature at 90% of strength)	°C	200	220	±200	±130 (matrix)	+ + ?	±130 (matrix)	0 tot + ?	±130 (matrix)
fire resistance	•	no	no	yes	yes	yes	yes	no	yes (matrix)
corrosivity in: – neutral concrete	•	– –	– –	+ +	+ +	+ +	+ +	+ +	+ +
– chloride concrete	•	– –	– –	+ +	+ +	+ +	+ +	+ +	+ +
– alkaline concrete	•	+ +	+ +	–	+	+ +	+ +	– – to –	to 0
electrical conductivity	•	+ +	+ +	none	none	+ +	+	none	none
EXECUTIONASPECTS (irrelevant for bare fibres)									
weight	g/cm3	7,9	7,9	(1,44)	1,25	1,77 to 1,96	?	2,6	?
flexibilty	•	–	–	•	+ +	•	–	•	–
anchoring	•	+ +	+ +	•	–	•	?	•	
vulnerabilty with transport/storage/execution	•	+	–	•	?	•	?	•	?

+ + very good
+ good
0 neutral
– bad

• irrelevant
? unknown
' estimated

* aramid 50% HM-fibre, 50% epoxy matrix
carbon 65% HTA-fibre, 35% matrix
glas 65% E-glasfibre, 35% matrix

4. COMPARISON OF THE PROPERTIES OF FRP ELEMENTS WITH REINFORCING STEEL

The properties which have to be looked upon first are the mechanical properties. Are the mechanical properties of FRP elements comparable to the properties of the normal reinforcing steel in order to be an alternative?

Aramid and glass FRP:

As a result of the relatively low E-modulus aramid (AFRP) and glass (GFRP) based FRP tensile elements are mainly fit to be used as prestressing material. The use of these elements as reinforcement would result in relatively large deformations and wide cracks. One could deal with this fact by increasing the fiber volume.

Carbon FRP:

The E-modulus of carbon based elements can be higher than of steel. However the deformation capacity of CFRP is very low compared to reinforcing steel because the plastic deformation of steel is lacking.

The different stress strain curves for steel, aramid carbon and glass are given in Fig. 4.3 of TASK 1.2.

As a result of this analysis the field of application of the FRP elements will be confined to the use as prestressing elements. Therefore in the following only the use of the elements as alternative for prestressing steel will be discussed.

5. COMPARISON OF THE PROPERTIES OF FRP ELEMENTS WITH PRESTRESSING STEEL

The items are discussed in the same order in which they appear in Table 3.2:

5.1 Shape; Diameter; Profile; Straightness

Design of FRP tendons with respect to geometrical appearance is strongly related to the prescriptions of manufacturers. It is possible to shape FRP in either rods, strips or strands, depending on the requirements of application. This is also true for the diameter. Experience shows that certain profiles are necessary to give the FRP prestressing tendons the desired properties for pre-tensioning. The fact that the FRP-tendons need to be profiled adds to the splitting force problem, which is related to the thermal expansion behaviour and the Poisson effect as well.

The idea is to start from the existing FRP tendons regarding geometrical shape. From the investigations it will be possible to conclude whether adjustments or alterations will be necessary.

5.2 Short-term Axial Strength

The short-term axial strength values of the different FRP types are more than sufficient in comparison to steel. Therefore no further investigation regarding this matter will therefore be necessary.

5.3 Long-term Axial Strength

This property is strongly related to other properties such as relaxation, fatigue, stress rupture, and corrosivity (since the environment always influences long-term properties). It will therefore be discussed for each FRP type in a special paragraph "durability" at the end of this chapter.

5.4 Radial Strength

In the case of aramid-based FRP the low radial strength restricts application possibilities to those where the FRP will not be subjected to direct transverse forces. For the other FRP this depends on the level of radial strength.

5.5 E-modulus (axial/radial); Strain at Failure; Elastic Strain; Deformation Capacity

As shown in Fig. 4.3 of Task 1.2 a fundamental difference between steel and FRP elements based on either aramid, carbon or glass is the shape of the stress-strain curve.

At a certain level of stress steel starts to show plastic deformation. This will be the case at overloading. If the load subsequently is removed the deformation will partly remain. If the FRP elements are overloaded and subsequently the load is removed these elements will return to their original shape.

The values of E-modulus and strain of the FRP are sufficient to be used as prestressing elements. Research will be based on the properties of the existing materials. Whether it will be necessary to alter these basic properties will follow from further application oriented research.

5.6 Poisson Ratio

Compared to the Poisson ratio of steel FRP in general have greater Poisson-ratios. This may lead to higher splitting forces (Hoyer effect) in the force transfer zone of pre-tensioned members which may reach the concrete tensile strength. Modifications will then be necessary to control this phenomenon.

5.7 Bending Capacity

In the case of prestressing applications this property has an execution vulnerability aspect but it is merely of significance for reinforcing steel and will therefore not be further discussed this document. When investigating the suitability of FRP for reinforced concrete it should however be kept in mind.

5.8 0,1 %-Strain Force; 0,2 %-Strain Stress; Constriction

These properties are deducted from specific requirements for prestressing and reinforcing steel. FRP show different strain behaviour than steel. Constriction of steel takes place during the plastic deformation part of the stress-strain curve, which is nonexistent with FRP. Constriction with respect to FRP is therefore not an item to investigate. Due to this absence of plastic deformation behaviour totally different criteria have to be applied to FRP in determining ultimate values up to where they can be responsibly prestressed. Following from the above no investigation is needed.

5.9 Interlaminar and Intralaminar Shear Strength; Transfer Length

The shear force transfer over the cross-section of a FRP element and its surrounding concrete can be modelled on the basis of Fig. 5.1 of the cross-section.

Fig. 5.1 shows that several discontinuities will be encountered. The core A is an anisotropic material consisting of fibers and matrix, whereas B and C will be considered more or less isotropic is this discussion.

Within A:

The force transfer between the fibers takes place by means of a resin. The quantification of this transfer can be referred to as **intralaminar** shear strength. This is an important property which must be further investigated.

Between A and B:

The quantification of the force transfer between the fiber containing core of the element and its coating, which may consist of either the same or a different resin, is referred to as **interlaminar** shear strength. This property will influence the transfer length, which may be an advantageous side effect, provided that the minimum steel requirements regarding transfer length will be met. Further investigation of this property is necessary.

Between B and C:

The force transfer between the element and the concrete/grout (resp. B and C) is quantified by the minimum length which is necessary to transfer a certain unit of force and reffered to as transfer length. Whereas most experimental transfer length determinations are based on "pull-out" tests the actual relevant behaviour should be determined by "push-in" tests, because the Poisson ratio works in favor of the bond to concrete in the case of a pretensioned FRP element. The results of pull-out tests have so far been satisfactory and since the push-in results will be even better no problems have to be expected here, except during failure of the FRP pretensioned concrete member. In that case the FRP element will be loaded beyond its pretensioning stress and the bond will be similar to the one during a pull-out experiment. Further investigation of this property is necessary.

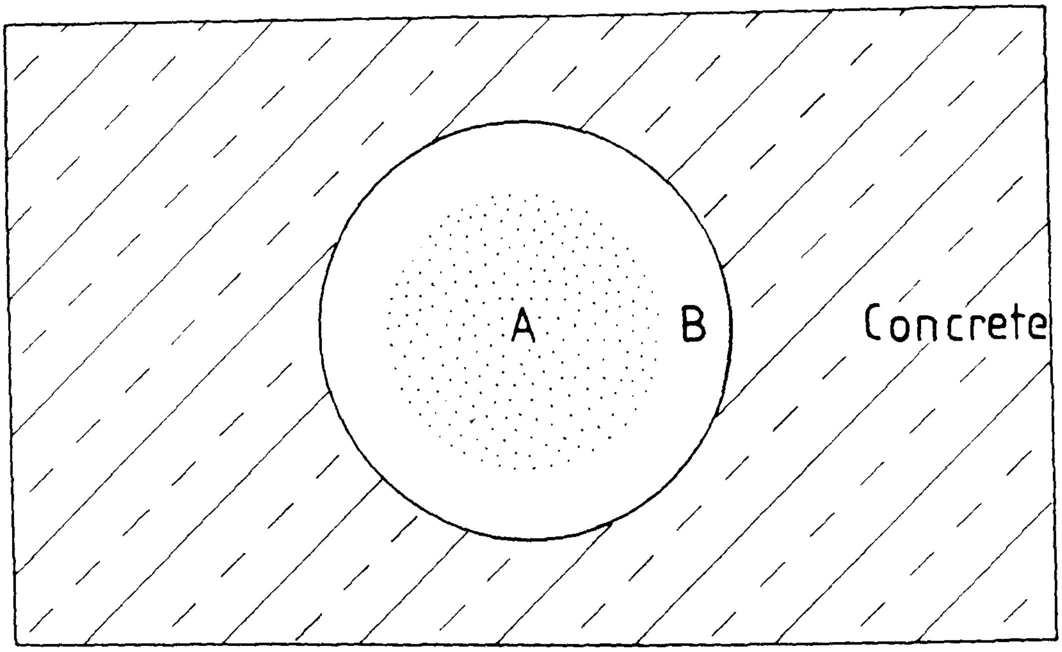

Fig. 5.1: Zones of Transfer of Shear Force in a FRP Element

5.10 Relaxation/Creep; Fatigue; Stress Rupture

These properties will be discussed for each FRP type in a special paragraph "durability" at the end of this chapter.

5.11 Thermal Expansion (Axial/Radial)

This aspect, recently discovered to be of utmost importance for FRP when applied as prestressing tendon in constructions with a thin concrete cover, was not recognised as a problem at the time of the formulation of the work program.

In the case of aramid-based FRP the radial thermal expansion coefficient is significantly greater than the axial one (which is even negative). The problem is that it exceeds the concrete thermal expansion coefficient substantially. Although the radial thermal expansion coefficients of the bare carbon and glass fibers are substantially lower than that of aramid it is their composite behaviour that counts. The resin applied to these FRP alternatives causes them to show a thermal expansion behaviour similar to aramid composites. This characteristic deserves great attention and requires thorough investigation.

5.12 Thermal Resistance; Fire Resistance

Exposure to very low temperatures does not lead to problems in the case of aramid-based FRP. Tests so far even indicated that the FRP-concrete bond is improved by it. Whether this is the case for the other FRP types is unknown.

The applied resins are thermo-setting so heating does not affect the composite properties negatively and therefore no specific vulnerability during storage or other execution stages has to be feared. The behaviour regarding fire resistance must however be investigated for applications where this is a requirement.

5.13 Corrosivity

See paragraph durability, where this item is discussed for each FRP type.

5.14 Conductivity

The conductivity behaviour is different for the FRP types, which results in a differing suitability for applications where specific conductivity characteristics are required.

5.15 Weight; Flexibility; Anchoring; Vulnerability; Toxicity

FRP are no health hazard and can easily be handled due to flexibility and low density.

In spite of a relatively low radial strength in the case of aramid-based FRP there are no reasons to believe that handling of FRP should take place with more care than prestressing steel. However this aspect must be looked at.

Neither difficulties with regard to concreting in humid conditions nor de-stressing problems are expected to occur. Extended exposure to ultraviolet light may affect FRP properties and must be investigated.

5.16 Durability

Durability of AFRP

The stress-rupture behaviour and the sensitivity of AFRP to an alkaline environment calls for new requirements. This is illustrated in Fig. 4.18 of Sub-Task 1.2, which shows the behaviour of a strip. The stress-rupture line represents the relation between the stress in a tensile element and the time that passes before the material fails under a specific sustained stress level. Of importance is also the residual tensile strength after a preceding long-term static force. The long term strength is also presented in Fig. 4.18. It can be seen that the residual strength of an unloaded strip after 100 years exposition to an alkaline environment like concrete is about 85 % of the short term strength. This value has been obtained by means of an extrapolation using the Arrhenius principle, that describes a relation between residual strength, temperature and time. Tests at elevated temperatures thus give indications about the residual strength under normal circumstances.

In assessing the structural safety one has to estimate the final prestressing level, taking into account all losses caused by the creep and shrinkage of the concrete and by relaxation of the FRP. This value must be compared with the characteristic stress-rupture curve.

Due to the non-corrosivity of FRP crack width is no design criterion unless for aesthetical reasons.

Durability of CFRP

The durability of CFRP in any kind of environment dangerous to steel is to be rated as excellent. CFRP are also superiour to the other kinds of FRP.

Durability of GFRP

The durability of GFRP elements when exposed to normal weather is superior to steel and equivalent to AFRP and CFRP. Chloride ions do not affect GFRP. Immediate contact with aqueons solutions of high alkalinity is however deletereous to GFRP. Such environments exist in fresh concrete and grout. Improvement becomes necessary by substituting the UP-matrices by EP-matrices in conjunction with special coatings. Further research is necessary.

Main Conclusions

The main conclusions are drawn by pointing out the important differences to reinforcing and prestressing steel by the way of comparison of FRP with the latter.

AFRP Elements

- better resistance to aggresive environments
- higher fatigue strength
- higher deformation capacity (low E-modulus)
- higher electrical resistivity
- non-magnetic
- fully elastic stress strain behaviour
- lower strain at failure
- higher creep and relaxation
- greater deformations (low E-modulus)
- thermal expansion behaviour very different from that of concrete

CFRP Elements

Most of the statements apply also for CFRP. But several differences must be pointed out:

- similar modulus of elasticity
- rather low ultimate strain
- superior corrosion resistance
- lower relaxation

GFRP Elements

Most of the statements made for AFRP with respect to the comparison with steel also apply for GFRP. The major differences to steel are:

- lower fatigue strength
- better resistance to aggressive external environment but less resistant when embedded in concrete or grout
- equivalent relaxation and creep

From these conclusions we can deduce that for post-tensioning applications all FRP seem fit. In pre-tensioning cases however the direct concrete contact is a problem for glass, due to alkaline corrosion. FRP on a carbon basis are, apart from being less economic than aramid-based FRP, interesting materials for pre-tensioning applications.

6. POTENTIAL FIELDS OF APPLICATION FOR FRP ELEMENTS

Based on the conclusions of chapter 5 the promising fields of use for the different FRP alternatives are given below:

6.1 Fields of Application for AFRP Elements

- As storage tanks resulting from its behaviour under low temperature conditions.
- As railway sleepers resulting from its excellent fatigue behaviour.
- As structural concrete members with very thin concrete cover due to its non-corrosivity.
- In defence transport industry due to its non-corrosivity.
- Inreligious/health/electronic apllications due to its non-corrosivity.

As a result of these conclusions, focus will be put on pre-tensioning with AFRP with ARAPREE. Possibilities for other FRP do however exist and therefore more or less parallel investigations must be carried out for all FRP where useful.

The application of Arapree will be investigated specifically within BRITE EURAM for the following applications:

- Pretensioned concrete elements for agro-applications which are exposed to severe corrosive environment.
- Balcony slabs, reinforced by Arapree-prestressed-bars.
- Railway sleepers
- Bank protection with the use of Arapree prestressed piles ("Perkoenpaaltjes") and shutters.
- Soil anchors
- Shutter shelves (e.g. as a substitution of tropical hardwood)

6.2 Fields of Application for CFRP Elements

Most of the potential fields of application presented for AFRP also seem to be open for CFRP. Because of their high modulus of elasticity which can be modified in such a way to be in the range of steel CFRP can be used for:

- Reinforcement for bending members and for secondary reinforcement
- Meshes

- Ground anchors in very aggressive soil and water
- Post-tensioning tendons, structural ties and stay cables

6.3 Fields of Application for GFRP Elements

As experience has shown GFRP high-strength tensile elements can be successfully used for:

- Tendons for the post-tensioning of concrete structures.
- Ground and rock anchors.
- Structural ties, stay cables.
- Incorporation of opto-electronic and electric sensors for supervision of structures.

SUB-TASK 1.2 REVIEW AND APPRAISAL OF THE PROPERTIES OF UD-FRP ELEMENTS AND THEIR PRODUCTION TECHNOLOGIES

1. SCOPE

All technical properties of FRP elements strongly depend on the properties of the components fiber and matrix. In consequence, at first the properties of suitable fibers and matrix materials have to be dealt with on basis of the literature and of the knowledge of the partners. Then a survey of commercially available FRP elements suitable for structural concrete and the state of the art on composite behaviour and experimental results is presented.

For the successful pursuit of the BRITE EURAM research and development work the presently available FRP elements and their production technologies are evaluated. The findings of SUB-TASK 1.2 are taken into consideration for the conclusions of SUB-TASK 1.1.

2. FIBERS AND MATRIX MATERIALS

2.1 Introductory Remarks

Fiber composites are being developed and used for a great variety of engineering applications. Several types of fibers and matrix materials have emerged. The types of fibers are: glass fibers, aramid fibers, carbon fibers, boron fibers, ceramic fibers and metallic fibers. For the production of linear tensile FRP elements for the purpose of prestressing and reinforcing of structural concrete only glass fibers, carbon fibers and aramid fibers have been successfully used up to now. Only these types of fibers will be dealt with furtheron.

Also the matrix materials show a great variety: polymer matrix, metal matrix, ceramic matrix. For the purposes dealt with in this report only polymer matrices are suitable: polyester, epoxy, and vinylester resin.

Finally, because of the application of FRP for structural engineering only the unidirectional arrangement of fibers within the polymer matrix is relevant.

2.2 Fibers for High-Strength Tensile Elements

2.2.1 Some Basic Requirements

Fibers for the manufacture of tensile elements in structural engineering must meet several basic requirements. From the structural point of view a high strength, a high modulus of elasticity and a sufficient elongation at the tensile fracture of fiber are necessary. Durability requires a high resistance to the environmental to which the structure will be subjected and also to the micro-environmental actions within the structural element (e.g. within the concrete).

Furthermore, the diameter of fiber should be as small as possible, because strength increases with diminishing fiber diameter. This requirement also leads to the increase of the so-called aspect ratio l/d which expresses the normalized necessary bond length for the transfer of force from broken fibers to unbroken fibers.

The following sections give a condensed overview on fibers suitable for unidirectional fiber composites for the reinforcement and prestressing of concrete. Their main properties and processes of manufacture are described in [2.1] and [2.2].

2.2.2 Glass Fibers

Glass fibers are widely used for the production of FRP. Common fibers are made of E-glass (≈ 55 % SiO_2; ≈ 8 % Al_2O_3; ≈ 19 % CaO; ≈ 5 % MgO). Stronger and more resistant to alkaline solutions, though more expensive than E-glass fibers, are fibers made from C- and S-glass (≈ 65 % SiO_2; ≈ 25 % Al_2O_3; 0 % CaO; ≈ 10 % MgO). The strength of glass fibers is dependent on the magnitude and density of surface defects which may be inflicted during handling etc. For the protection of the fiber its surface is treated immediately after fiber drawing with a thin polymeric coat compatible with polymeric matrices. This coat also improves the bond with the matrix.

Glass fibers are round, with the diameter ranging from 5 to 25 μm. Fig. 2.1 shows the array of glass fibers in a FRP-element. Table 2.1 contains some global information on the tensile strength and Young's modulus. The producers cited in Table 2.1 are given as examples. Glass fibers are purely elastic up to failure.

2.2.3 Aramid Fibers

Aramid fibers are synthetic organic fibers, called aromatic polyamide fibers. They are a polycondensation product of terephthaloyl chloride (TCD) and p-phenylene diamine (PPD). The chemical structure is shown by Fig. 2.2. Aramid fibers have an anisotropic structure of high crystallinity, consisting of cross-linked chains of macromolecules. The molecular chains are aligned and rigidified by means of aromatic rings linked by hydrogen bridges.

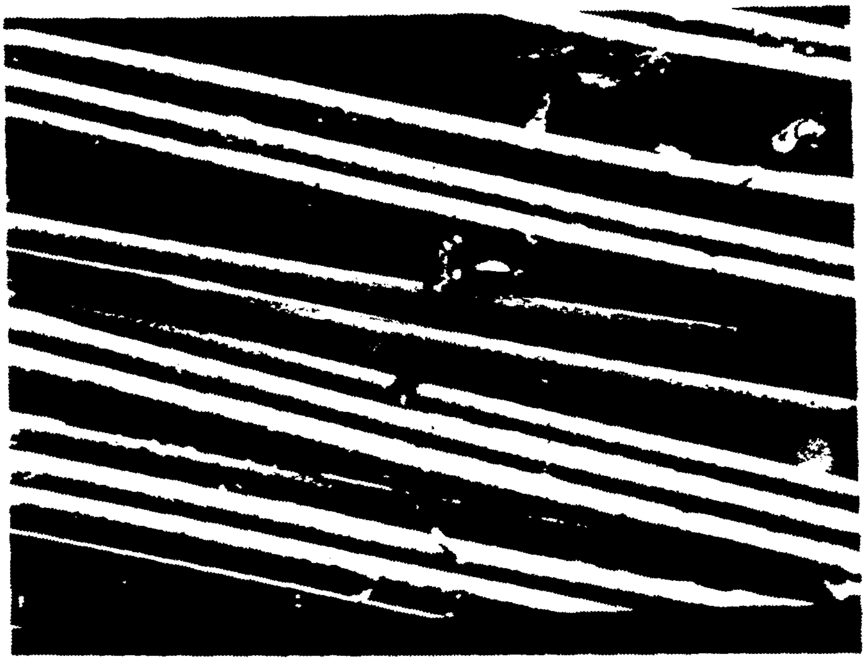

Fig. 2.1: Array of Fibers in Composite

Table 2.1: Common Fibers (Global Information)

type of fiber	denomination or brand name	tensile strength f_f	mod. of elasticity E_f	producers (examples)
		kN/mm^2	kN/mm^2	
glass	E-glass	1,67	51	Bayer AG
	S-glass	4,58	87	Owens/Corning Fiberglas
aramid	Twaron	2,80	125	Aramide Maatschappij
	Kevlar	2,65	128	Du Pont
carbon	Carbon HP; HS	3,0	300	Hysol Grafil
	Tenax	3,6	230	Enka/Nippon Carbon Co.

There are three main producers of high performance aromatic polyamide fibres worldwide: Dupont in the U.S. (Kevlar-aramid), Aramide Maatschappij v.o.f. in the Netherlands (Twaron-aramid) and Tejin in Japan (Technora-aramid). There are three types of Twaron-aramid: Normal, Intermediate and High Modulus (NM, IM and HM) and two types of Kevlar: Kevlar 29 and Kevlar 49. An overview of the properties of the aramid fibers is given in Table 2.2. Aramid fibers have a high tensile strength in axial, i.e. chain direction by strong covalent bonds while the transverse strength is lower due to the weaker hydrogen bonding of cross-linkage. The diameter of the fiber is in the range of 12 μm.

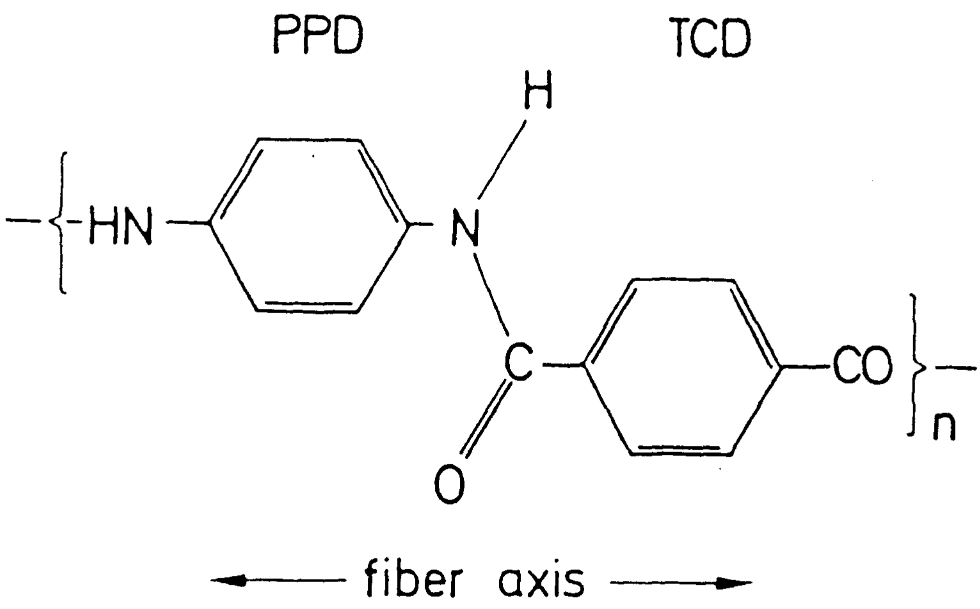

Fig. 2.2: Chemical Structure of Aramid

2.2.4 Carbon Fibers

Although the names "carbon" and "graphite" are used interchangeably when relating to fibers, there is a difference. Typically, PAN (polyacrylonitrile)-base carbon fibres are 93 % to 95 % carbon by elemental analysis, whereas graphite fibres are usually more than 99 % carbon. For applications as high-strength fiber composite tensile elements we consider mainly carbon fibers. The basic difference between these two types relates to the temperature at which the fibers are heat-treated. PAN-base carbon is produced at about 1300 °C, while higher modulus graphite fibers are graphitized at 2000 to

3000 °C. Graphite fibers have high strength and very high moduli. These properties remain constant at high temperatures.

A basic disadvantage of the use of carbon fibers for high strength fiber composite tensile elements in structural engineering is their cost. They still are by volume about 7 to 10 times more expensive than steel. The raw materials, or precursors, for PAN-base fibers are expensive, and the processes of carbonization and graphitization consume much time, energy and materials and require close control throughout.

Some producers and some brand names of carbon fibers are given in Table 2.1. Table 2.3 shows several properties of HM (high elastic modulus) and HT (high tenacity) carbon fibers. For the application of such fibers for tensile elements an adequate ultimate strain at fiber fracture is essential. Carbon fibers are highly corrosion resistant. Their diameter is in the range of 5 to 10 μm.

2.2.5 Comparison of Fibers

The fibers treated here are compared with each other and with high-strength prestressing steel with respect to selected properties for the application. Fig. 2.3 compares the σ_f-ϵ_f-lines of several fiber types. In Table 2.4 several properties of FRP are compared with each other and with high-strength, colddrawn prestressing steel.

Table 2.2: Some Properties of Aramid Fibers

property	unit	Twaron			Kevlar		Technora
		NM	IM	HM	29	49	
density	$g \cdot cm^{-3}$	1,44	1,45		1,44	1,45	1,39
tensile strength	MPa	3000			3000		3000
Young's modulus	GPa	70	85	125	63	130	70
ultimate strain	%	3,6	3,2	2,3	4,0	2,3	4,4
coeff. therm. exp. $\parallel$	$10^{-6} \cdot K^{-1}$	- 3,5			- 3,5		?
coeff. therm. exp. $\perp$	$10^{-6} \cdot K^{-1}$	60			60		?
decomposition temp.	°C	500			500		500
elt. conductivity	10^{15} Ωcm	7			7		?

Table 2.3: Some Properties of Carbon Fibers

type	density	short-term tensile strength	Young's modulus	ultimate strain
	g/cm^3	GPa	GPa	%
HM 300	1,8	4,0	300	1,3
HM 400	1,8	2,7	400	0,6
HM 500	1,9	2,4	500	0,5
HT 3.6	1,7	3,6	230	1,5
HT 4.5	1,8	4,5	250	1,8
HT 5.6	1,8	5,6	300	1,8
HT 7.0	1,8	7,0	300	1,8

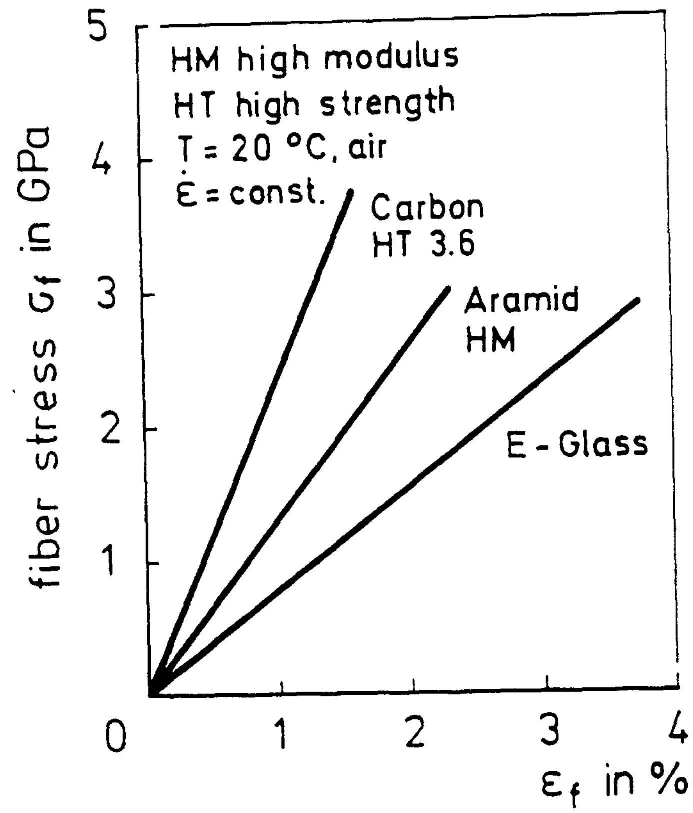

Fig. 2.3: Stress-Strain Lines of Various Fibers

2.3 Matrix Materials

The matrix materials for FRP used for tensile elements are polymers. Most commonly used are the thermo-setting polyester and epoxy resins. In the future also thermoplastic polymers may become of interest. The matrix has to serve several purposes. All fibers dealt with here exhibit a high axial tensile strength but a pronounced sensitivity against lateral normal stress. Thus, the matrix has to protect the fibers from local transverse effects and from abrasion. The ingress of moisture, detrimental media and light is impeded by the matrix. An ideally parallel arrangement of fibers within the ud-FRP renders the highest axial tensile strength. This presupposition cannot be fully met however. Hence the matrix has to equalize the force distribution by deviatory pressure and interfacial shear. Upon approaching failure of the FRP tensile element fibers will commence to break. It is the task of the matrix to transfer the force of broken fibers to unbroken ones by interlaminar shear.

Table 2.4: Comparison of Properties of Various Fibers with Prestressing Steel

	Fiber			Prestr.
Property	Aramid	Carbon	E-Glass	Steel
tensile strength	++	++	++	+
long-term strength	0	++	0	+
fatigue strength	++	+	-	+
multiaxial strength	-	0	-	+
durability in:				
alkaline environment (like concrete)	0	++	-	++
aggressive acidic environment	+	++	+	-
carbonated concrete	++	++	++	-
weight	++	++	+	-

classification from poor (-) to excellent (++)

Polyester is the most widely used matrix, especially for GFRP (glass FRP). Polyester resins exhibit adequate resistance to water, many chemical agents, weathering and ageing. Their cost is low. More expensive are epoxy resins which in many respects have a better performance than polyester resins [2.1]. Resins may absorb water and swell, which may lead to a loss of strength of the FRP.

In the range of service temperatures of concrete structures of about $-30\ °C \leq T \leq 60\ °C$ the resins are in the glassy state. In this state they exhibit an approximate linear stress-strain behaviour under short-time load, whilst being viscoelastic under long-term stress. The glass-transition temperature is between 120 and 140 °C. Their tensile strength is in the range of 40 to 100 MPa, the Young's modulus is in the range of 2 to 5 GPa. The coefficient of thermal expansion exceeds that of the fibers markedly: 80 to $100 \cdot 10^{-6}\ K^{-1}$.

It has to be pointed out that microcracks in the resin matrix may arise when using FRP elements for prestressing (1 to 1,5 % strain). This may have adverse effects on the durability of the FRP. Matrix resins with ultimate tensile strains of 4 to 6 % are desirable.

The behaviour of a composite is also influenced by the interface between fiber and matrix. The flow of force between fiber and matrix requires adequate interfacial bond [2.1]. Bond can be classified in mechanical and chemical bond. Mechanical bond (shear key effect) seems not to be very efficient. Chemical bond and adhesion by wetting are the more important effects. They are enhanced by coupling agents and the surface sizing or treatment of fibers.

2.4 Literature

[2.1] Chawla, K. K.: Composite Materials. Science and Engineering. Springer-Verlag, New York, 1987.

[2.2] Tsai, S. W. and Hahn, H. T.: Introduction to Composite Materials. Technomic Publ. Co. Westport Conn./USA, 1980.

3. SURVEY OF COMMERCIALLY AVAILABLE FRP ELEMENTS

3.1 Scope

The FRP tensile elements dealt with here are ud-composites of fibers which are fully embedded in epoxy or polyester matrices. They can be utilised for the reinforcing and/or prestressing of structural concrete. In addition, they can be applied for ground and rock anchors, for structural ties and other purposes.

FRP elements are not standardized, neither on national nor on international levels. Hence, it will become necessary to mention brand names and producers of FRP to give the interested reader the opportunity to contact producers for further information. It should be noted that the overview on types, brand names and producers of FRP is unbiased and incomplete. The literature sources [3.1] to [3.11] present an overview on the use of AFRP, GFRP and CFRP for the reinforcement and prestressing of concrete.

3.2 Shapes

Most of the FRP tensile elements have either a circular or rectangular cross-section (round bars or flat strip). Diameter of round bars are typically in the range of 4 to 10 mm. Flat strips have cross-sectional areas of up to 150 mm^2.

FRP elements used for the pre-tensioning of concrete members may be surface-treated to improve bond. The surface may be: sand-coated, shaped or knurled.

FRP elements are produced by a continuous process. They may be coated on-line with a polyamide or polypropylene coat for additional protection. Table 3.1 gives an overview on products. In addition to compact FRP elements, recently also strands with seven and more CFRP wires were developed.

3.3 Production Technologies

Nowadays in principle two different technologies are applied for the production of unidirectional fiber composites. The most common technology is pultrusion. The often applied prepreg method is used for the production of multidirectional and plain composites.

3.3.1 Pultrusion

A sketch of the pultrusion process is given in Fig. 3.1. The single production steps can differ considerably from producer to producer, but the principle is valid in every case.

1 - the required amount of fibers is taken from coils.
2 - the fibers are impregnated with a thermo-setting resin.
3 - a shape is given to the wet fiberbundels.
4 - the impregnated fibers are cured.
5 - material transport is done by pulling the cured product.
6 - the FRP is cut in length.

Typical modifications of the above mentioned standard process are:

a - resin impregnation takes place in the shaping die (combination of step 2 and 3)
b - by the use of fiberprepregs instead of bare fibers the online resin impregnation (step 2) is dropped.
c - at Fibra a braiding of the fibers takes place (between step 1 and 2). Since the shape is more or less fixed by this means, an additional shape giving (step 3) is redunant.

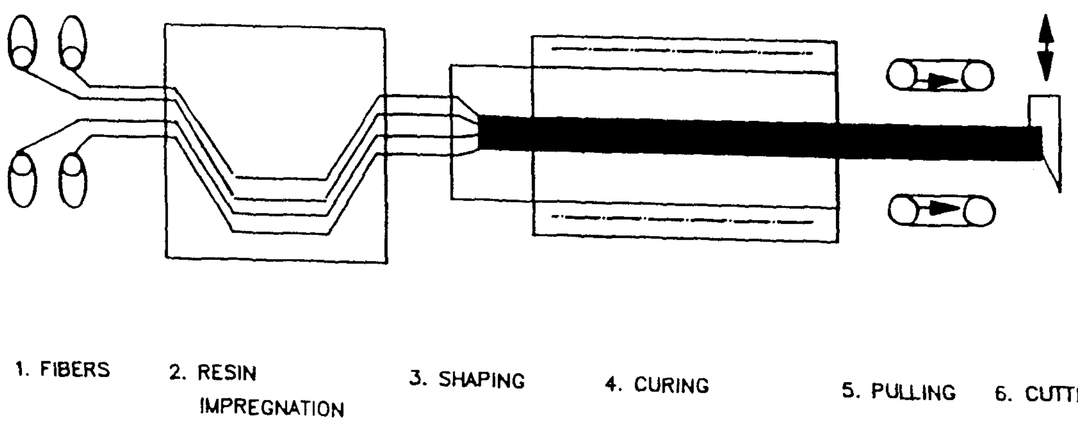

Fig. 3.1: Pultrusion Technology

Usual process parameters of pultrusion and dimensions of the products are:

production speed:	0.5 m/min ÷ 2.0 m/min
cross-section	: round, flat, multishaped
surface	: smooth
size	: 1 mm ÷ 50 mm

3.3.2 Prepregging

The manufacturing process of FRP by means of the prepreg method is described for the material CFCC (see Fig. 3.2), since this is the only product using this technology on a commercial scale.

1 - fibers are (separately from the other production steps) impregnated by using special prepreg-resinsystems. These resins cure very slowly and further processing is possible within some months. This intermediate product is called fiber prepreg.

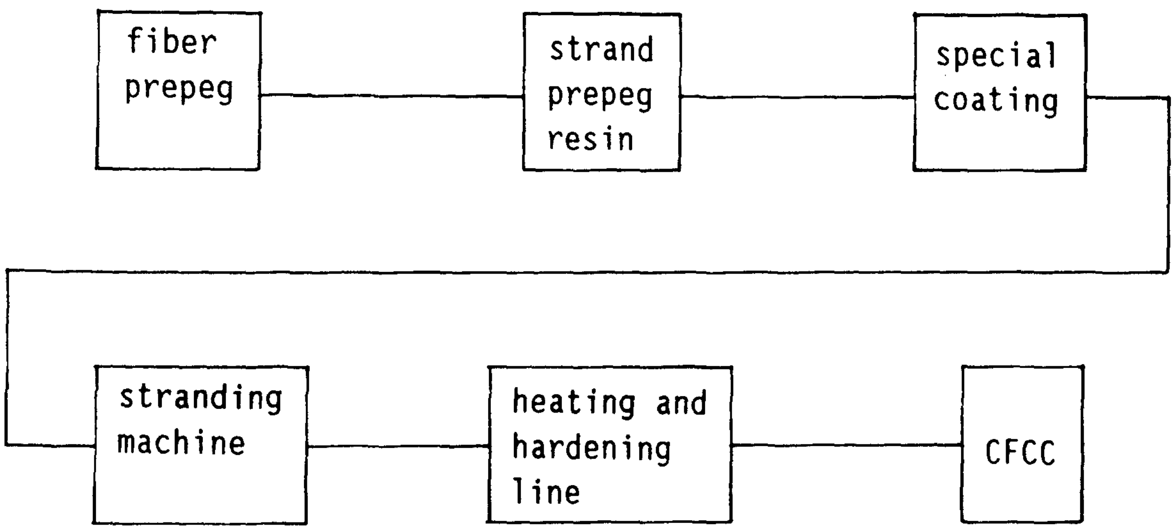

Fig. 3.2: Manufactoring Process of CFCC

Table 3.1: Several Manufacturers of FRP for Civil Engineering Applications

manufacturer	country	fiber	matrix	brandname
Akzo	NL	A,C	EP	Arapree
Arisawa	J	A,C,G	EP	
Bayer AG	D	G	UP	Polystal
Bridon Composites	GB	A,C,G	EP,UP	Bri-ten
Cousin	F	G	UP	JONCS JT
IMCO	USA	G	UP	
Kuraray	J	PVA	EP	
Mitsubishi Kasei	J	C	EP	Leadline
Mitsui constr.	J	A	EP	Fibra
Polygon	USA	G	EP	
Pultrall	CAN	G	UP	Isorod
Sportex	D	G	EP	
Teijin	J	A	VE	AFRP rod
Tokyo rope	J	C	EP	CFCC

A = aramid, C = carbon, G = glass, PVA = polyvinylalcohol,
EP = epoxy, UP = unsaturated polyester, VP = vinylester

2 - by stranding plural pieces of fiber prepregs, a piece of strand prepreg is fabricated.

3 - the surface of the strand prepreg is treated by special coating and turned into a composite linear body.

4 - plural composite linear bodies are stranded and turned into a composite stranded body.

5 - the composite stranded body is finally heated and hardened.

The process parameters of the CFCC production and the dimensions of the products are:

production speed: 0.5 m/min (estimated)
cross-section : round
surface : slightly structured
size : 1.3 mm ÷ 40 mm

The following comparison of the above mentioned production technologies comprises only economic and technological items. A comparison of the material properties is given later.

Table 3.2: Comparison of FRP Production Technologies

characteristic	pultrusion	CFCC prepreg method
production speed	o	-
prodcution costs	+	++
shape diversity	++	+
size diversity	+	++
surface formation	--	+
matrix option	+	--
product quality	++	+

(high++,+,o,-,--low)

3.4 Overview on FRP-Elements

At present an actual overview on commercially available FRP high-strength tensile elements for the reinforcement and prestressing of concrete is rather difficult. This is due to the dynamic development of the market, partly also often due to scant information available.

Table 3.3: High Strength Fibrous Tensile Elements (Examples)

tensile element	type of fiber	fiber brand name	type of composite	producer
AFRP	aramid	Technora	vinyl-ester bonded bar	Teijin (Jap)
Arapree	aramid	Twaron HM	parallel fibers in epoxy resin	AKZO (NL)
CFCC	carbon	-	epoxy-bonded bar and seven wire strand	Tokyo Ropes (Jap) and BASF (D)
Fibra-bar	aramid	Kevlar 49	epoxy-resin impregnated braided rod	Mitsui, Shimizu (Jap)
Nefmac	glass aramid carbon	various	resin impregnated	Nefcom, Shimizu (Jap)
Parafil	aramid	Kevlar 49	bare parallel fiber in sheating	ICI (UK)
Polystal	glass	E-glass	polyester-bonded bar	Bayer and Strabag (D)

Table 3.3 presents an incomplete list of FRP elements. It should be mentioned that Parafil is not a FRP. In Table 3.4 the properties of several commercial products are presented. The values of the tensile strength and of the modulus of elasticity relate to the fiber cross-section and to the composite section as well. Hence when comparing products, the fiber volume must be taken into consideration.

Table 3.4: Comparison of some FRP Properties

material (brandname or manufacturer)	fiber/ matrix -	V_f Vol.-%	tensile strength f.r./c.r. MPa	Young's modulus f.r./c.r. GPa	ultimate strain %	relaxation/ load level % of F_u t in [h]	bond str. to concr. MPa
Arapree	A/EP	45	3000[a)] 1350	123[a)] 55	2.3[a)]	7/55/100 20/55/10^6 [b)]	7.5
Arisawa	C/EP	53	3000 1590	235 125			
Polystal	G/UP	68	2455 1670	75 51	3.3	1,4/47/100 3/50/5x10^5 [c)]	0.8
Bri-ten	G/UP	65	2385 1550	78 51	3.0		
Joncs JT	G/UP	61	2785 1700	72 44	3.8		
Leadline	C/EP	65	2790 1815	229 149	1.3	2,5/70/100 3,8/70/10^6 [d)]	
Fibra	A/EP	59	2350[a)] 1380[a)]	110[a)] 65[a)]	2.0	9/50/100	8.2
Polygon	G/EP	60	2990 1790	93 56	3.1	6/50/10^6	
AERP rod	A/VE	65	2865 1865	81 53	3.7		
CFCC	C/EP	64	3290[a)] 2120[a)]	213[a)] 137[a)]	1.6[a)]	2/80/100	7.2

f.r. = related to the effective fiber cross-section; c.r. = related to the composite cross-section; a = mean value
b/c/d = value extrapolated from test data of 27,000/1,500/100 hours;

Table 3.4: (continued)

material (brandname or manufacturer)	stress-rupture MPa/time in h	fatigue $N/F_o/F_u$ MPa	density t/m^3	coeff. therm. exp. (parallel) $10^{-6}/K$	Poisson ratio -	ILSS MPa
Arapree	$1650/10^6$ a,e)	$>2x10^6$/ 2000/1600	1.25	-1.8	0.38	45a)
Arisawa						
Polystal	$1650/5x10^5$ a)	$2x10^6$/ 1080/920	2.0	7.0		35a)
Bri-ten				2.0	7.0	
Joncs JT					1.95	
Leadline		$2x10^6$/ 2025/200	1.57	0.7		
Fibra		$>2x10^6$/ 1090/645		-5.2		
Polygon			2.0		0.27	79
AERP rod				1.3		
CFCC		$>2x10^6$/ 2045/1565		0.6		

a = mean value; b/c/d = value extrapolated from test data of 27,000/1,500/100 hours; e = test in sat. Ca(OH) + 0.4 n KOH)

3.5 Literature

[3.1] Dolan, C.W.: Developments in Non-Metallic Prestressing Tendons. ACI-Journal, Sept.-Okt. 1990, pp. 80/88.

[3.2] Iyer, S.L.; Kumaraswamy, C.: Performance Evaluation of Glass and Fiber Composite Cable for Prestressed Concrete Units. 33rd Int. SAMPE Symp., Anaheim, March 1988, pp. 844/851.

[3.3] Kakihara, R.; Kamiyoshi, M.; Kumagi, S.; Noritake, K.: A New Aramid Rod for the Reinforcement of Prestressed Concrete Structures. ASCE Spec. Conf.: Advanced Composites Materials in Civil Engineering Structures, Las Vegas, 1991, pp. 132/142.

[3.4] Les matériaux nouveaux pour la précontrainte et le renforcement d'ouvrages d'art. Int. Symp. ENPC, Paris, Oct. 1988.

[3.5] Mießeler, H.-J.; Wolff, R.: Experience with the Monitoring of Structures Using Optical Fiber Sensors. FIP-XIth Int. Congress on Prestressed Concrete, Hamburg, June 1990, pp. Q 12/17.

[3.6] Mikami, H.; Katok, M.; Takeuchi, H.; Tamura, T.: Shear Behaviour of Concrete Beams Reinforced with Braided High Strength Fiber Rods in Spiral Shape. FIP-XIth Int. Congress on Prestressed Concrete, Hamburg, June 1990, pp. T 44/46.

[3.7] Gerritse, A.; Maatjes, E.; Schürhoff, H.J.: Prestressed Concrete Structures with High-Strength Fibers. IABSE Report Vol. 55, Zürich, 1987, pp. 425/432.

[3.8] Gerritse, A.; Schürhoff, H.J.; Maatjes, E.: Prestressed Concrete Structures with Arapree; Relaxation. IABSE-Symp. Concrete Structures for the Future, Versailles, 1987.

[3.9] Reinhardt, H.W.; Gerritse, A.; Werner, J.: Arapree - A New Prestressing Material is Going into Practice. FIP-XIth Int. Congress on Prestressed Concrete, Hamburg, June 1990, pp. T 66/69.

[3.10] Rostásy, F.S.: New Materials for Prestressing. FIP-Symp., Jerusalem/Israel, Sept. 1988.

[3.11] Rostásy, F.S.; Budelmann, H.: FRP-Tendons for the Post-Tensioning of Concrete Structures. ASCE Spec. Conf.: Advanced Composites Materials in Civil Engineering Structures, Las Vegas, 1991, pp. 155/166.

4. STRENGTH AND DEFORMATION OF FRP

4.1 Scope

The design and structural detailing of r/c- and/or p/c-members, reinforced and/or prestressed with FRP tensile elements, requires adequate knowledge of the mechanical properties of fiber composites. FRP are generally unfamiliar materials to structural engineers, who are used to work primarily with isotropic or at least with quasi-isotropic materials. FRP are orthotropic. Their mechanical behaviour depends markedly on the state of stress and also on temperature, environment, strain history etc. The main features of the mechanical behaviour will be described in the following sections.

4.2 Mechanical Behaviour Under Short-term Loading

4.2.1 Basic Relations

For the prediction of the properties and of the behaviour of a composite the so-called rule of mixtures often is a useful tool. Thereby the properties of the FRP are considered as the volume-weighted average properties of the components. In the rule of mixtures the following subscripts are used: f, m, c and p denote fiber, matrix, composite and voids, respectively. The masses, volumes and densities of the components and of the composite are given by the following equations:

$$V_f = \frac{M_f}{\rho_f}$$

$$V_m = \frac{M_m}{\rho_m} \qquad (4.1a \text{ to } 4.1d)$$

$$V_c = V_f + V_m + V_p$$

$$M_c = M_f + M_m$$

These expressions can be normalized:

$$v_f = \frac{V_f}{V_c}; \; v_m = \frac{V_m}{V_c}; \; v_v = \frac{V_p}{V_c}; \qquad (4.1e)$$

$$v_c = v_f + v_m + v_v = 1$$

$$m_f = \frac{M_f}{M_c};\ m_m = \frac{M_m}{M_c};\ m_p = 0 \qquad (4.2a\ \text{to}\ 4.2c)$$

$$m_c = m_f + m_m = \frac{\rho_f}{\rho_c} v_f + \frac{\rho_m}{\rho_c} v_m \qquad (4.2d)$$

The density of the composite can be expressed as follows:

$$\rho_c = \rho_f v_f + \rho_m v_m \qquad (4.3)$$

4.2.2 Elastic Constants and Composite Stresses

In Fig. 4.1a the ud-element is subjected to in-plane stresses. The composite axial stress σ_c may be devived under the presupposition that the components and the composite will undergo an identical axial elastic strain [4.1]. With the rule of mixtures we obtain:

$$\sigma_c = \sigma_f v_f + \sigma_m v_m = \sigma_f v_f + \sigma_m (1-v_f) \qquad (4.4)$$

The axial composite Youngs's modulus E_c and the Poisson's ratio μ_c are:

$$E_c = E_f v_f + E_m v_m = E_f v_f + E_m (1-v_f) \qquad (4.5)$$

$$\mu_c = \mu_f v_f + \mu_m v_m = \mu_f v_f + \mu_m (1-v_f) \qquad (4.6)$$

The Eq.(4.4) to (4.6) presuppose the elastic behaviour in the fiber direction irrespective of the stress magnitude. For practical purposes this presupposition is justified for high-strength FRP because the contribution of the fibers is far greater than of the matrix and because the fibers are ideally elastic. This fact is shown for the GFRP Polystal ø 7,5 mm bar in Fig. 4.2.

For stresses σ_{cn} acting perpendicular to the fiber axis the assumption $\sigma_{cn} = \sigma_m = \sigma_f$ leads to the transverse modulus of elasticity of the composite (Fig. 4.1b):

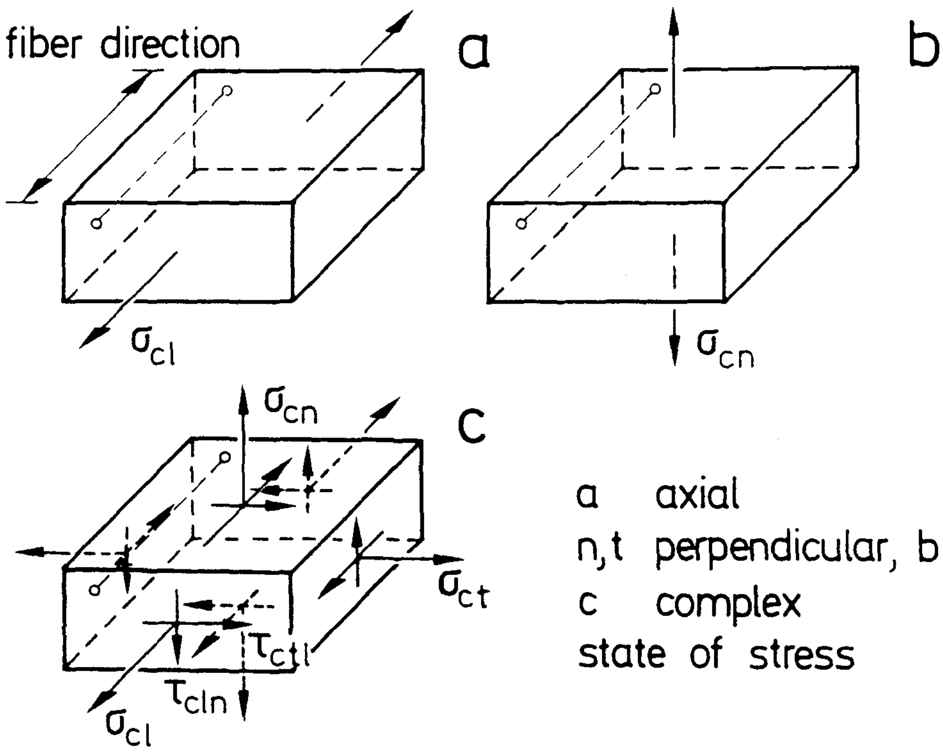

Fig. 4.1: In-Plane Stresses in UD-FRP Element

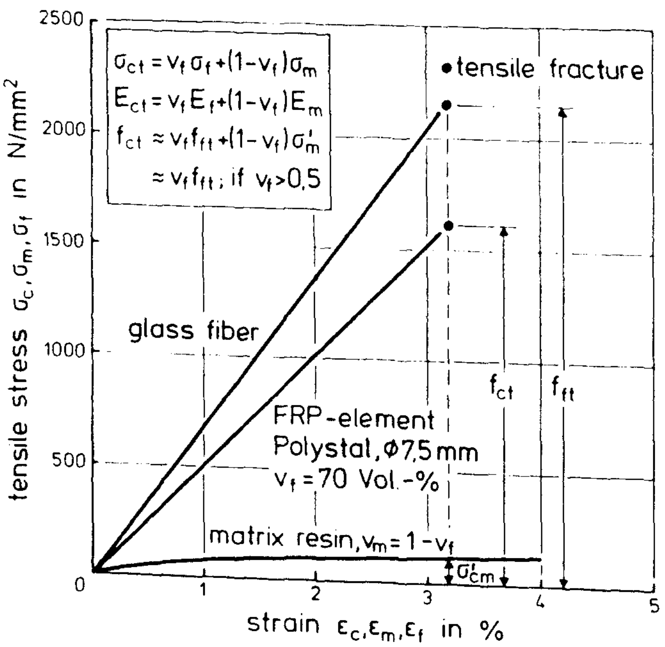

Fig. 4.2: Rule of Mixtures for Polystal Bar

$$E_{cn} = E_m \frac{1}{v_m + v_f \frac{E_m}{E_f}} \tag{4.7}$$

Because for the FRP treated here the modulus of fibers considerably exceeds the modulus of the matrix, $E_f >> E_m$, the transverse modulus of the FRP corresponds essentially to the isotropic Young's modulus E_m of the matrix.

It should be pointed out that even for the ud-composite the rule of mixtures is only an approximation of the complex micromechanical behaviour [4.1].

4.2.3 On Strength and Fracture Under Short-Term Loading

4.2.3.1 Axial stress-strain line and axial strength

For the use of the FRP element for a tendon or structural tie etc. its axial composite strength is especially of interest. With Fig. 4.2 the axial tensile strength can be written as

$$f_{ct} \approx f_{ft} \, v_f + \sigma_m{}' \, v_m \tag{4.8}$$

with $\sigma_m{}'$ the adjunct stress of the nonlinear behaviour of the matrix at the attainment of the ultimate strain of fiber ε_{fu}. Because the fiber is much stronger than the polymeric matrix the contribution of the matrix to the axial strength is generally negligible. Thus, we may write.

$$f_{ct} \approx f_{ft} \cdot v_f \tag{4.9}$$

The compressive composite strength σ_{cc} in fiber direction is of no relevance for the FRP's use as tensile unit. It may become important for the tendon-anchorage assembly.

Fig. 4.3 depicts the composite stress-strain lines of several commercially available FRP elements. They are compared with the σ_p-ε_p line of a high-strength, cold drawn, stress relieved prestressing wire. Stress-strain behaviour of FRP is practically ideal-elastic and brittle. It must be noted that the fiber content v_f is different for the elements shown. Thus, both fiber content and fiber properties must be known to forecast the property of the composite. The force of the FRP element may be written:

$$F_c = \sigma_c \, A_c \tag{4.10}$$

The definition of composite stress as shown is in line with the civil engineering custom for isotropic materials. Hence, it is also proposed to define the strength of FRP by the number and total cross-section A_f of fibers and by the fiber strength:

$$F_c \approx \sigma_{ft} \, A_f \tag{4.11}$$

Clearly, both definitions are equivalent if the strength is forecast with Eq. (4.9).

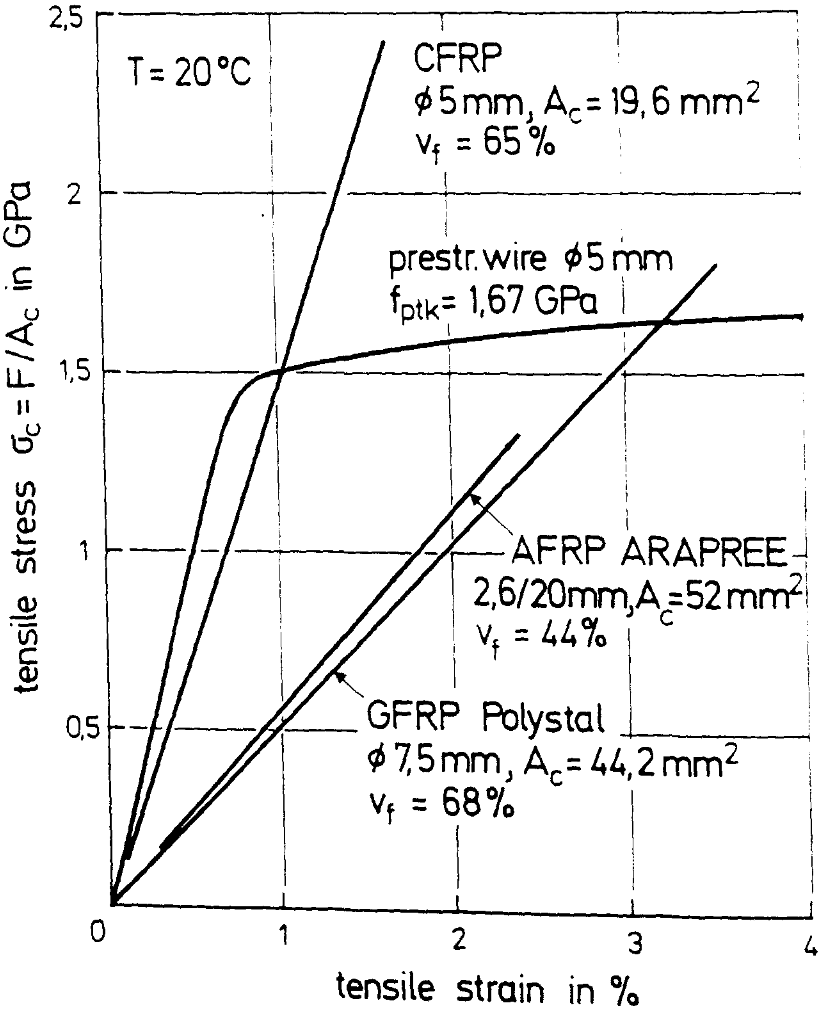

Fig. 4.3: Stress-Strain Lines of Various FRP Elements

4.2.3.2 Multiaxial strength

The application of FRP as tendon requires the transfer of the axial tensile force to the anchorage or in case of pre-tensioning directly to the concrete of the structure. Transfer and anchorage of tensile force lead to a change from the uniaxial state of composite stress to a multiaxial one. Besides axial stresses σ_c, also transverse stresses σ_{cn} and also shear stresses τ_c act on the surface and in the interior of the FRP element (Fig. 4.1c). Hence, the effect of multiaxial stress on strength behaviour becomes relevant.

For the FRP available today little is known about their multiaxial stress-strain relations, especially taking into consideration the variation of thickness and properties of the matrix layer over the FRP's cross-section. Therefore, Fig. 4.4 only gives a qualitative impression of the multiaxial strength envelope for the ud-layer subjected to planar stresses [4.2, 4.12 and 4.13]. Fig. 4.4 shows a cut-out of the failure envelope for tensile composite stresses σ_{ct}, as compressive stresses σ_{cc} are generally irrelevant. Only the upper symmetrical half of the "truncated cone" is depicted. Stress combinations within the cone are carried without failure, those outside or on the cone's surface lead to failure. It can be shown that the resultant axial strength will be markedly influenced by simultaneous shear and perpendicular stress. Without generalization, examples of the other strength values are given for a ud-GFRP: E-glass; v_f = 45 %; epoxy matrix; as percentage of the true tensile strength f_{ct}: $f_{cnt} \approx 3$ %; $f_{cnc} \approx 11$ %; $f_{cs} \approx 7$ %; $f_{cc} \approx 57$ %; [4.2].

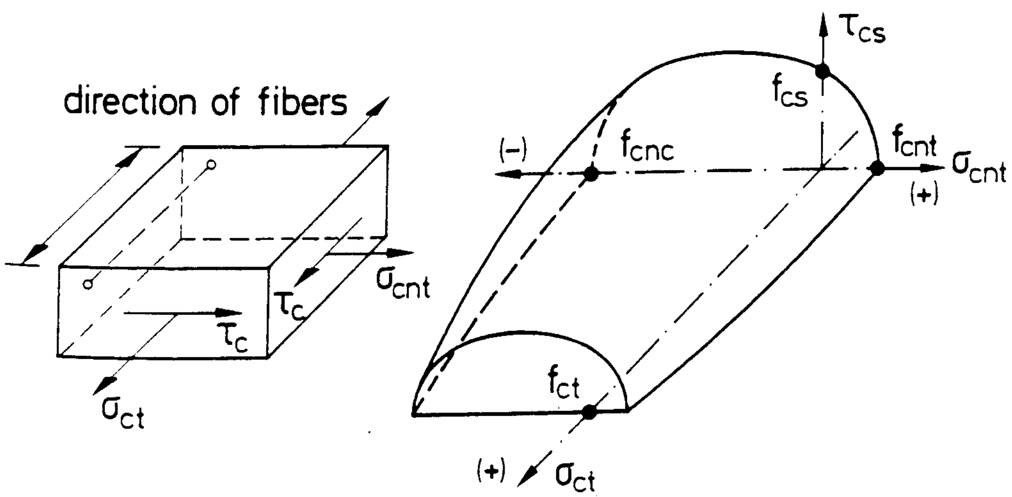

Fig. 4.4: Failure Envelope of UD-Layer Under Planar Stresses

4.2.3.3 Modes of fracture

As described in [4.1] the mode which determines the failure of the specific ud-FRP in short-term axial loading depends on several parameters. These parameters are to be sought in the microstructural influences of the composite and in the properties of components. The microstructure comprises the following items: type, diameter of fiber, fiber volume, distribution and parallelism of fibers, fiber defects and fiber distribution; matrix and interfacial relations to fiber; etc.

In order to ascertain composite action up to failure of the FRP in tension, the matrix must have a greater ultimate strain ε_{mu} than the brittle-elastic fiber ε_{fu}: $\varepsilon_{mu} > \varepsilon_{fu}$. When approaching failure individual fibers will break because of the variability of defects, and hence also of the strength along the fiber's length. As Fig. 4.5 shows this event will lead to interfacial slip between the broken fiber and the matrix on the one hand and to a stress magnification in adjacent fibers on the other hand. Due to the still effective interfacial bond a gradual build-up of tensile stress in the broken fiber along the bond transfer length will take place. If the interfacial bond strength is exceeded, delamination of fiber from the matrix will commence and propagate from the broken end of the fiber. With interfacial bond lost, progressive fiber fracture will occur, thus leading to overall failure.

This cumulative type of failure has been treated theoretically by several authors, taking into account the statistical variation of fiber strength. In [4.1] an overview is presented.

The assumption of a straight σ_c-ε_c-line up to failure of the ud-FRP is an approximation of reality. Fig. 4.6 shows that the cumulative damage process will cause jumps of the σ_c-ε_c-line due to fiber breaks near the maximum load.

4.2.4 Influence of Temperature on Strength and Deformation

4.2.4.1 Practical relevance

In structural components of automotive vehicles and aircraft elevated temperatures of $\geq$ 150 °C are rather usual during regular service. This is not the case in normal civil engineering structures. The range of temperature a structural concrete member will experience during service is largely a matter of the ambient climate. This range may be assumed to be: -30 °C $\leq$ T $\leq$ 80 °C. In addition to such moderate service temperatures, extraordinary, high temperatures as in case of fire and their effects on FRP materials are of interest.

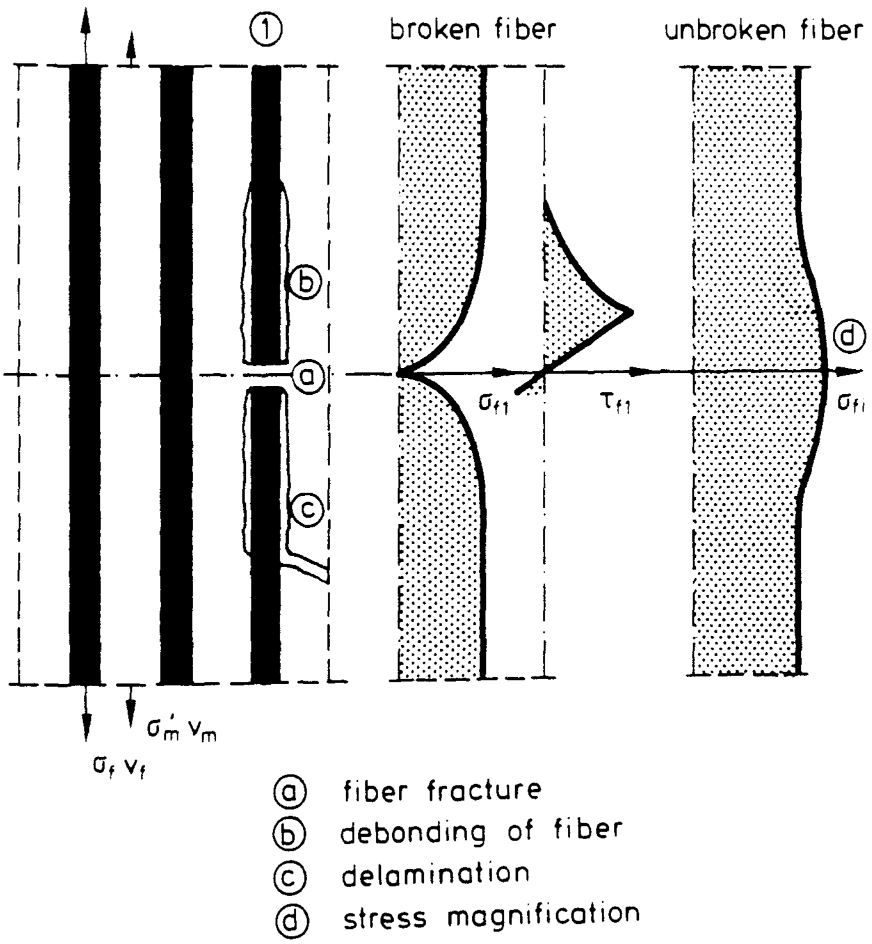

Fig. 4.5: Modes of Fracture

With FRP being composite materials consisting of a strongly temperature dependent matrix resin and of fibers which are less affected by temperature, the temperature dependence of various properties can be expected to be significant. The effect of temperature on the coefficient of thermal expansion in relation to the component expansion and anisotropy is treated in sec. 6.2. Here, the effects on the tensile strength and on the modulus of elasticity will be described.

4.2.4.2 Influence of temperature on the tensile strength of the components

The influence of temperature on the tensile, short-term strength of the fibers dealt with here is qualitatively shown in Fig. 4.7 [4.3]. Within the above-mentioned range of temperature the tensile fiber strength is not markedly affected. Negative temperature leads to an increase of strength of aramid and glass fibers. Beginning with 150 °C, both types of fiber exhibit an accelerating loss of strength, while carbon fibers, tested in an inert atmosphere, are not significantly influenced by temperature. Generally, the duration of temperatures ≤ 100 °C has no marked influence.

Fig. 4.7 also shows that aramid and glass fibers will not sustain at a very high temperature, e.g. in the case of fire. Carbon fibers will incinerate at extremely high temperatures.

The influence of elevated temperature on the matrix resin is far more pronounced than on the fibers. Because elevated temperature decreases the modulus of elasticity and strength and, furthermore, causes time-dependent deformation, the glass transition temperature T_g, must be distinctly above the maximum service temperature. For temperature resistant polyester and epoxy resins, the glass transition T_g is in the range of 130 to 140 °C.

4.2.4.3 Influence of temperature on composite strength and elasticity

The type of matrix resin and its volume content v_m are of influence. Fig. 4.8 shows test results for GFRP [4.4]. Strength decreases with temperature. It is interesting to note that the residual strength at 20 °C of heated and stressed GFRP is higher.

The relative change of Young's modulus in axial tension of several FRP is shown in Fig. 4.9. Again, CFRP reacts very insensitively to temperature.

4.2.5 Influence of Moisture on Strength and Deformation

4.2.5.1 Practical relevance

As described in sec. 6.3, FRP materials may absorb water dependent on the relative humidity of the surrounding air or from the material the FRP element is in contact with. The absorption of water of GFRP and CFRP only occurs within the polymer matrix. In AFRP a certain amount of water can be

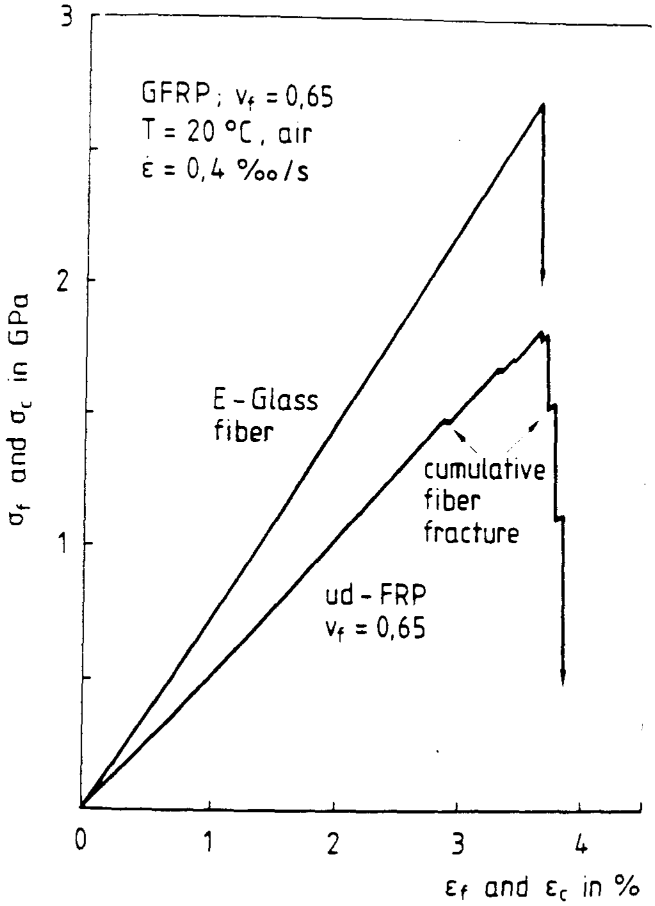

Fig. 4.6: Cumulative Damage

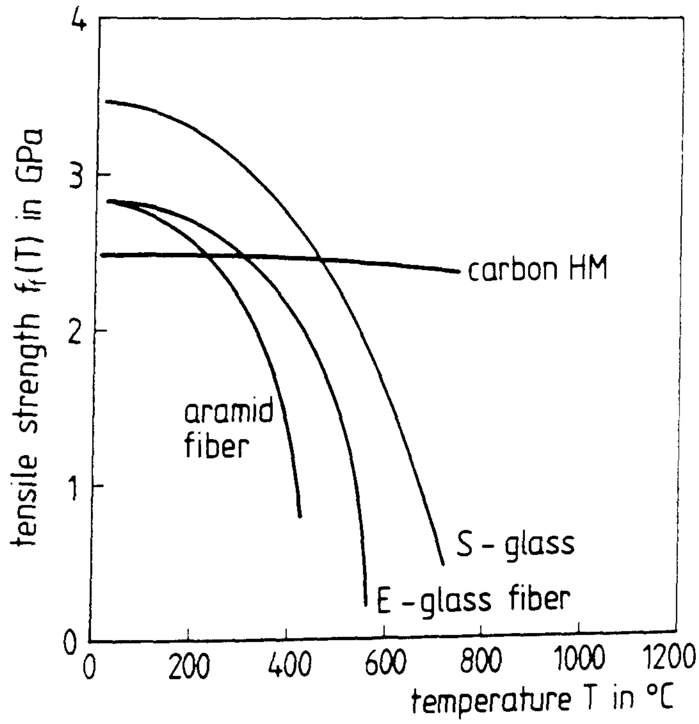

Fig. 4.7: Influence of Temperature on Fiber Strength

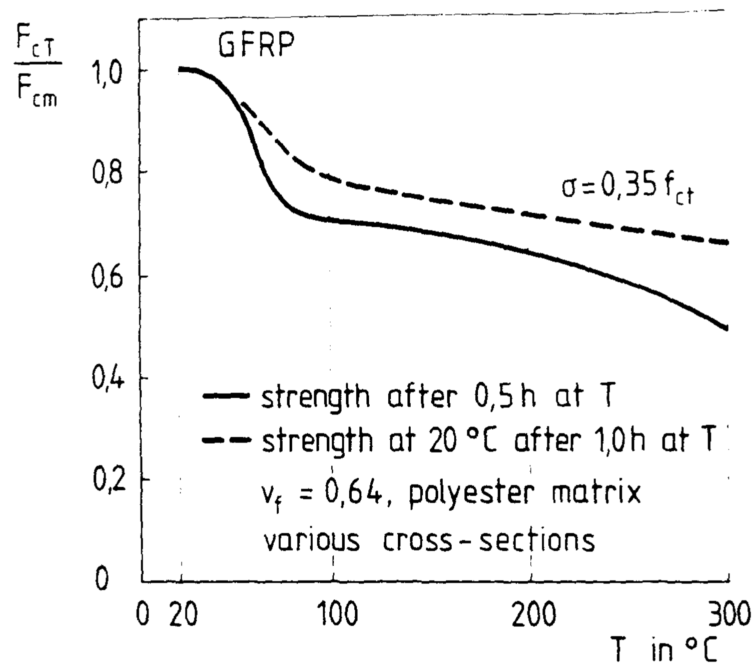

Fig. 4.8: Influence of Temperature on Tensile Strength of GFRP Bars

Fig. 4.9: Change of Young's Modulus due to Temperature for Various FRP

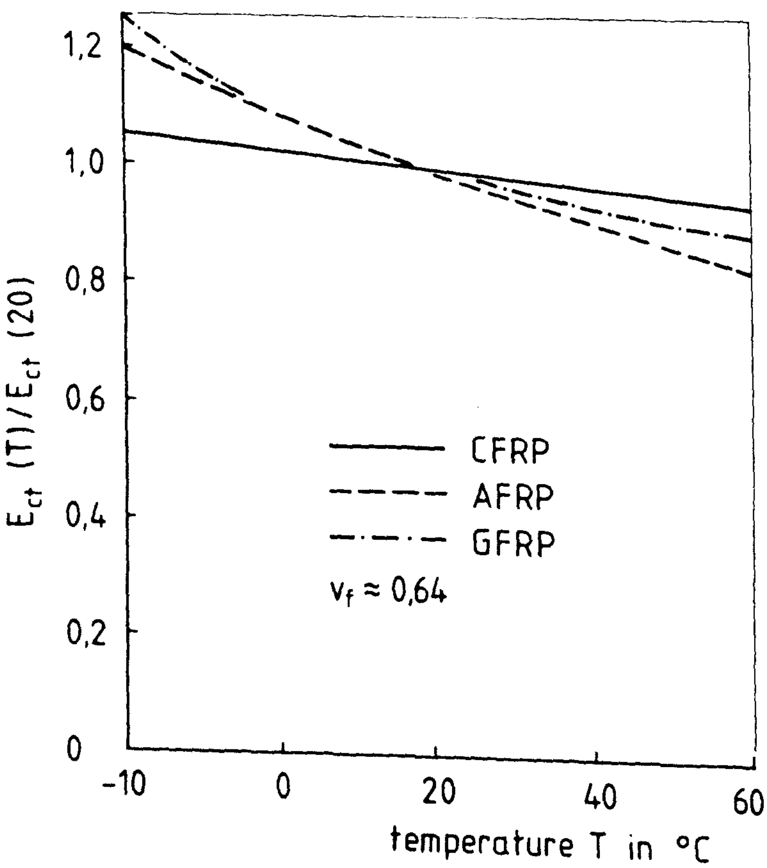

absorbed by the aramid fiber. The absorption of water is a slow process tending towards the mean equilibrium moisture content m_{eq} which depends on the surrounding climate. Once m_{eq} is attained, e.g. after 1000 h, variation of moisture will be slow and small. For practical application, the equilibrium moisture content must be known because of its influence on strength and elasticity. It is important to note that the absorption of water and its influence on mechanical properties are entirely reversible processes.

4.2.5.2 Influence of moisture on composite behaviour

The effect of moisture on the strength and elasticity of FRP materials must be sought in the fact that moisture lowers the glass transition temperature T_g of the polymer matrix. Immediately after manufacture, the FRP element does not contain any evaporable water. It will then pick-up moisture during storage. Thus, for strength testing the moisture content must be known.

Taking the day of fabrication as reference time, the apparent decrease of strength in a defined climate vs. storage time can be established. For GFRP, $v_f \approx 0{,}68$, a decrease of 4 to 6 % of the virgin strength was measured for a storage in a climate of 20 °C/65 % r.h. (relative humidity). The Young's modulus will only be slightly affected.

4.2.6 Ageing due to Radiation

If FRP elements are exposed to solar radiation without protection and for a prolonged duration a significant loss of strength will occur. This loss of strength is caused primarily by ultraviolet radiation which, after an initial insignificant increase of strength due to supplementary crosslinkage in the matrix resin, reverts to degradation due to chain breaking. Degradation is enhanced by oxygen and moisture. Fig. 4.10 shows this degradation for several ud-FRP materials dependent on the accumulated ultraviolet radiation energy per cm^2 surface area [4.3]. The degradation of GFRP is less pronounced than for AFRP and CFRP. This observation is not due to a special sensitivity of aramid and carbon fibers against radiation but to the greater thermal and hygroscopic expansion incompatibility between these fibers and their matrix resin in contrast to glass fibers and the epoxy matrix. This mismatch may lead to microcracking in the matrix and to debonding. The conclusion can be drawn that FRP must be shielded from ultraviolet light.

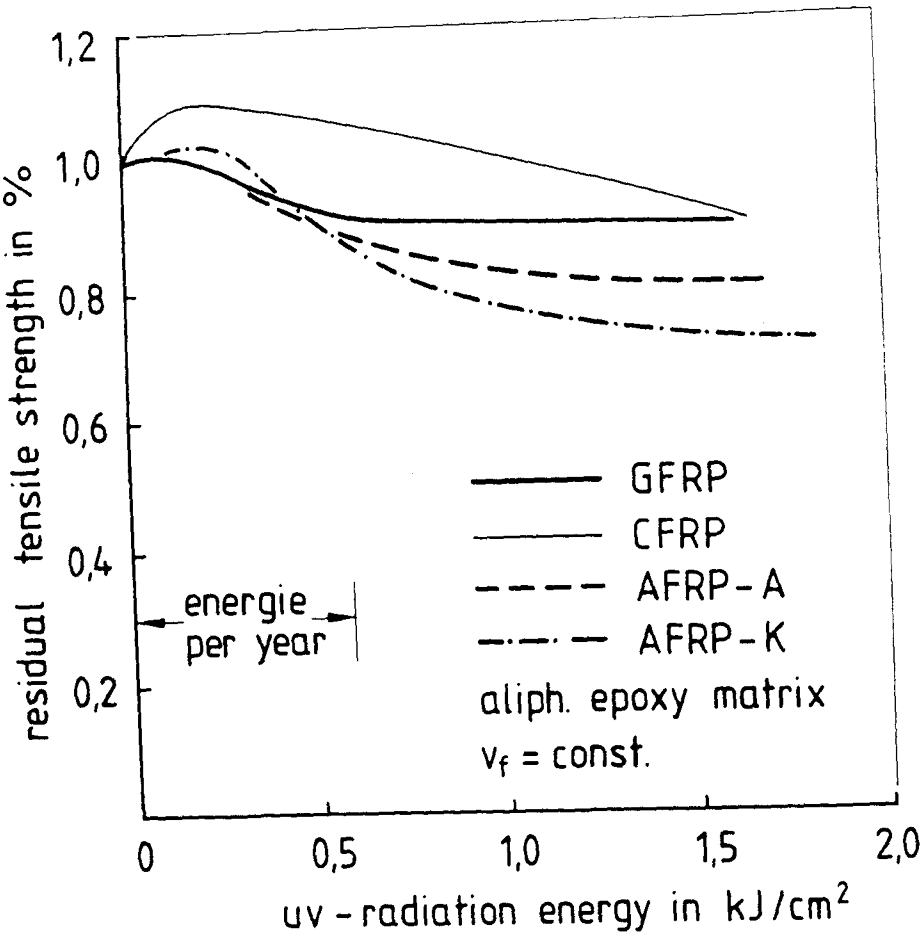

Fig. 4.10: Degradation of Strength of Several UD-FRP Due to UV-Radiation

4.2.7 Variability of Strength

4.2.7.1 Practical relevance

Fibers and composites are brittle materials. Therefore, their strength must be expressed by statistical means. The variability of the strength of fibers is dealt with, dependent on the number of fibers in a bundle and on the length of fibers [4.1]. This variability is relevant for the strength of fiber bundles not embedded in a matrix. It can be shown that the mean strength of fibers embedded in a matrix is considerably higher than that of the identical number of non-embedded fibers. Exactly this observation led to the development of FRP. It is due to fact that, in a ductile matrix, the propagation of cracks initiated from fractures of individual fibers is markedly impeded. For engineering purposes these problems are not very important because they are implicitly included in the measured strength of the composite element. Here the influence of the length and number of FRP elements on the strength of a tendon or tie is an important question which will be dealt with below.

4.2.7.2 Influence of length of FRP element on strength

The tensile strength of FRP elements of a certain cross-section A_c, fiber content v_f, etc. is tested with specimens of a certain length l_0. Statistical evaluation of test results with a suitable probability density function $f(x_1)$, will lead to the cumulative probability of failure $F_1(x_1)$. With x_1 the strength of the FRP element with the length l_0 is notated. The strength x_1 is a scattering property.

A FRP element with a greater length, $l > l_0$, can be regarded as a chain of i links, with $i = l/l_0$. For this chain the failure probability can be expressed by

$$F_i(x_i) = 1 - [1 - F_1(x_1)]^i. \tag{4.12}$$

The probability density function of the chain is the derivative of the failure probability Eq.(4.12):

$$f_i(x_i) = i\ f_1(x_1)\ [1 - F_1(x_1)]^{i-1}, \tag{4.13}$$

which must be known to express the effect of the length of the FRP element on its strength. For the probability density function the so-called Weibull-formulation can be chosen:

$$f_1(x_1) = m \left(\frac{x_1}{x_0}\right)^{m-1} \cdot \frac{1}{x_0} \cdot \exp\left[- \left(\frac{x_1}{x_0}\right)^m\right] \tag{4.14}$$

For the probability of failure we then obtain:

$$F_1(x_1) = 1 - \exp\left[- \left(\frac{x_1}{x_0}\right)^m\right] \tag{4.15}$$

In the Eq.(4.14) and (4.15), m and x_0 are the so-called Weibull parameters which have to be determined experimentally. An example of the procedure is shown in [4.5].

Now for the FRP element of the length $l = i \cdot l_0$, with $i \geq 1$ the number of unit elements l_0 in l, we obtain the probability density function and the probability function:

$$f_i(x_i) = i\, m \left(\frac{x_i}{x_0}\right)^{m-1} \cdot \frac{1}{x_0} \exp\left[- i \left(\frac{x_i}{x_0}\right)^m\right] \quad (4.16)$$

$$F_i(x_i) = 1 - \exp\left[- i \left(\frac{x_i}{x_0}\right)^m\right] \quad (4.17)$$

For any chosen failure probability $F^* = F_i = F_1$, the ratio of strength of FRP elements with the length l and l_0 can be expressed:

$$\frac{x_i}{x_1} = i^{-\frac{1}{m}} \quad (4.18)$$

The length dependence of strength does not depend on the chosen failure probability but only on the length of the FRP element and on the Weibull parameter m. For small values of the standard deviation σ_1 of the tensile strength x_1, tested on specimens with the length l_0, the parameter m can be expressed by the coefficient of variation V_c of the population x_1. With

$$V_c \approx \frac{\sigma_1}{x_1} \quad (4.19)$$

the parameter m can be expressed as:

$$m \approx \frac{1}{V_c} \quad (4.20)$$

Tests on GFRP bars by [4.6] show the length dependence of the tensile strength in Fig. 4.11. The length of specimens was varied in the tests, $l \leq 5$ m. The solid line represents the median relative strength derived in [4.6], the dashed line represents Eq. (4.18) for the ratio of median strengths (median value: failure probability = survival probability). The decrease of strength is relevant especially for unbonded tendons, but not for FRP tendons bonded in grout or concrete. It has to be pointed out that this effect is valid for any type of material, also for prestressing steel.

4.2.7.3 Strength variability in unbonded tendons

Unbonded tendons are composed of a plurality of n individual tensile elements, all of them having the same length $l = i \cdot l_0$. Thus, such arrangement can be looked upon as a series of parallel chains, each with i links. With the tools derived in sec. 4.2.7.1 the maximum attainable rupture force F_{cu} can be related to the median strength x_l or to the characteristic short-term strength x_{lk} of FRP material as determined by tests on short specimens l_0. We obtain for the median strength (ln, natural logarithm):

$$\frac{F_{cu}}{n \cdot \check{x}_l} = \frac{F_{cu}}{\check{F}_c} = i^{-\frac{1}{m}} \cdot (m \ln 2)^{-\frac{1}{m}} \cdot \exp\left\{\frac{1}{m}\right\} \tag{4.21}$$

and for the characteristic strength (5 %-fractile):

$$\frac{F_{cu}}{n \cdot x_{lk}} = \frac{F_{cu}}{F_{ck}} \approx \frac{m}{m-1{,}645}\, i^{-\frac{1}{m}} \cdot (m \ln 2)^{-\frac{1}{m}} \cdot \exp\left\{\frac{1}{m}\right\} \tag{4.22}$$

Both equations (4.21) and (4.22) were evaluated with the test results obtained from tests with single unit GFRP elements, Fig. 4.11. These tests gave a value of $m \approx 46$ [4.6]. Fig. 4.12 shows the evaluation for the cable. As can be expected, the strength of the cable is reduced in comparison to the single unit tendon of the length $l = i\, l_0$.

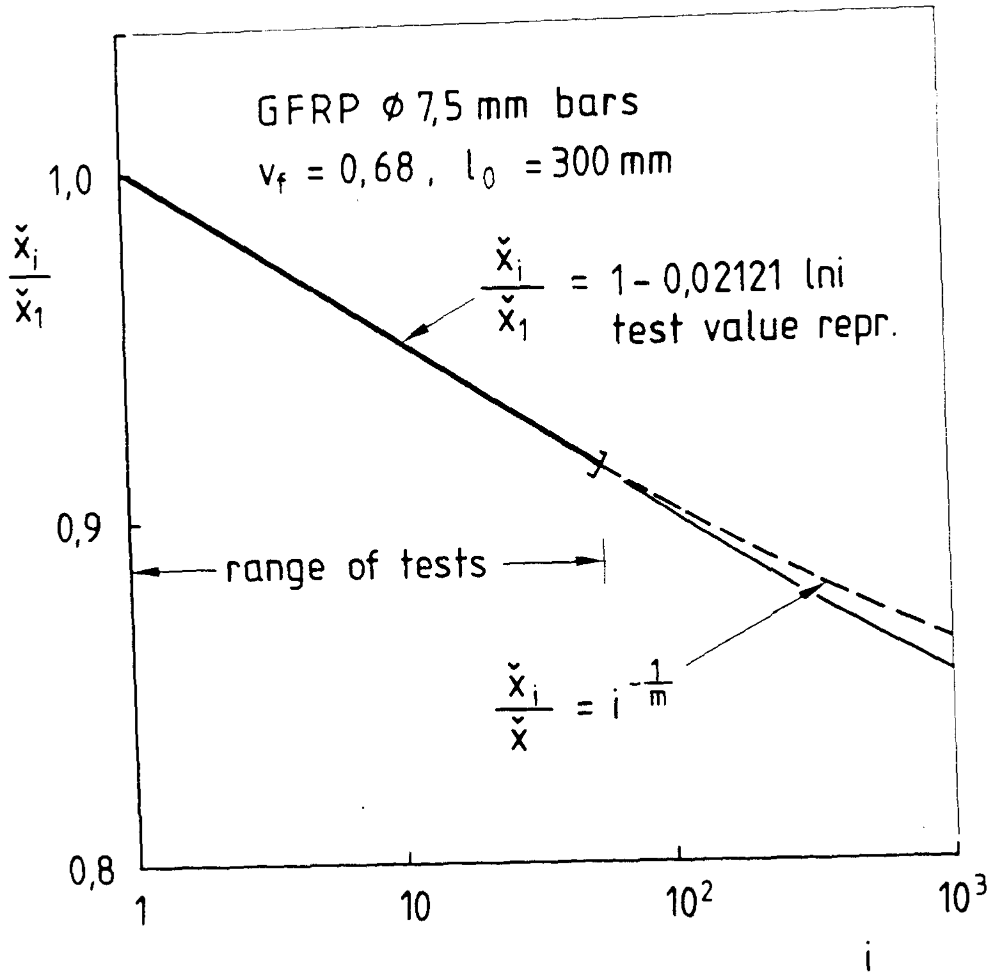

Fig. 4.11: Length Dependence of Strength of GFRP Bars

4.2.8 Characteristic Axial Short-Term Strength, Test Procedures

For the design of prestressed concrete members the permissible axial tensile stress or the corresponding permissible force of the FRP element has to be expressed in terms of the characteristic force $F_{ck} = f_{ck} \cdot A_c$ which has to be determined on basis of tensile tests with the FRP element. In these tests, the specimen has to be gripped in such a way that the true strength of the FRP material can be obtained with a break in the free length.It should not be concealed that the development of a suitable laboratory anchorage which fulfills the before-mentioned requirement is a difficult task. It cannot be stressed enough that this is a highly important problem. An unsuitable anchorage leads in essence to a "waste" of the tensile potential of the FRP and hence to economical disatvantage.

Tests show that the FRP material exhibits its highest strength immediately after production, i.e. at its minimum moisture content. Storage at normal conditions, e.g. 20 °C/65 % r.h. leads to a small, though reversible reduction of strength which is reached after 1 to 2 weeks of storage. Consequently, tensile testing should be performed after such a preconditioning of the FRP material. Certainly if the FRP element is to be used in a different environment, e.g. entailing high moisture content or high alkalinity, this must be also investigated.

The force F_{ck} or the axial short-term strength f_{ck} is determined by statistical evaluation of the test results of an adequate sample size (n > 30). The probability density of strength can be assumed to be Gaussian. The force F_{ck} is defined as 5 %-fractile of the total population.

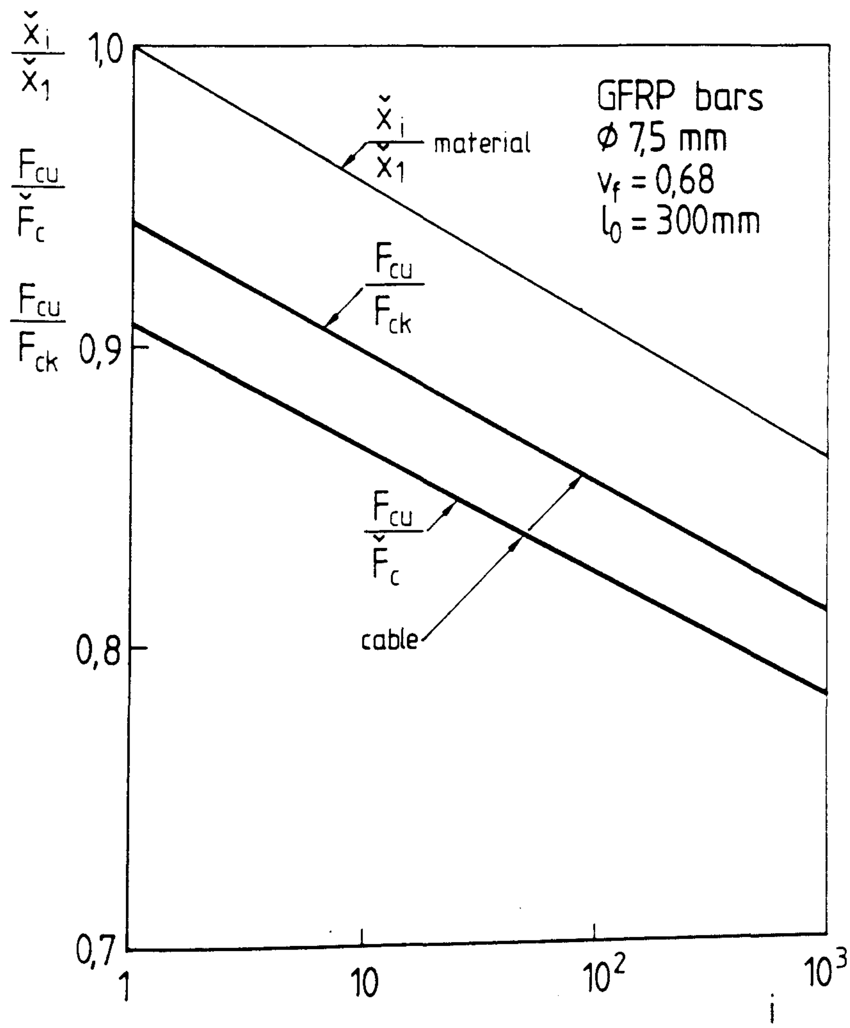

Fig. 4.12: Length Dependence of Strength of Cables

4.3 Mechanical Behaviour Under Sustained Loading

4.3.1 Practical Relevance

FRP elements used as reinforcement, as tensile units for the pre-tensioning of prefabricated concrete members, or as tendons for post-tensioning are primarily subjected to long-term static stresses. Certainly, stress variations will superimpose this more or less constant stress level. During sustained loading the FRP element is also subjected to the relevant environment of the structure and possibly also to the specific concrete environment (e.g. pH 13). Furthermore, temperature variations may occur.

Experiments show that long-term static stresses may reduce the tensile strength of FRP, with the environmental condition being an important influence. The admissible permanent tensile stress of the FRP must take into consideration the phenomena of creep rupture strength and strength retention. In a p/c-structure the initial prestress will decrease in course of time. Besides, creep and shrinkage of concrete also the creep and relaxation of the tendon material must be taken into account.

The phenomenon of creep rupture is irrelevant for prestressing steel if the permissible stress does not exceed $\sigma_{pmo} \leq 0{,}75\ f_{ptk}$, provided reliable protection against corrosion is secured.

4.3.2 Mechanism of Creep Rupture

4.3.2.1 Endurance

For the experimental assessment of the tensile creep rupture behaviour of a specific FRP element, the specimens are subjected to a constant force and to an invariant environment (Fig. 4.13):

$$F_{cl} = \text{const} \leq F_{cu}$$

F_{cu} is the relevant short-time static tensile rupture force of the specimen tested which in fact is unknown. The force F_{cl} can be endured for the time t_u at which creep rupture occurs. Prior to failure at t_u, microcracks in the matrix followed by debonding will occur. The final phase of rupture is accompanied by a rapid growth of damage. The time-dependence of the total

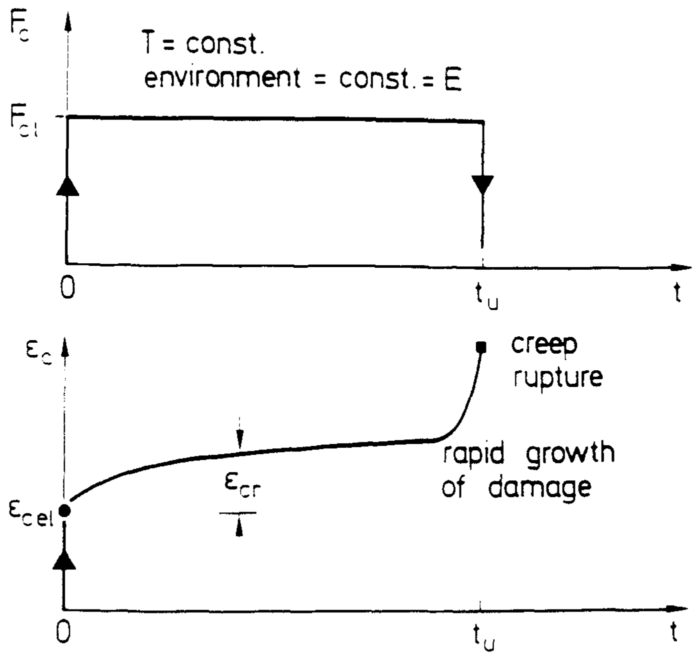

Fig. 4.13: Time-Dependence of Force and Strain in the Creep Rupture Test

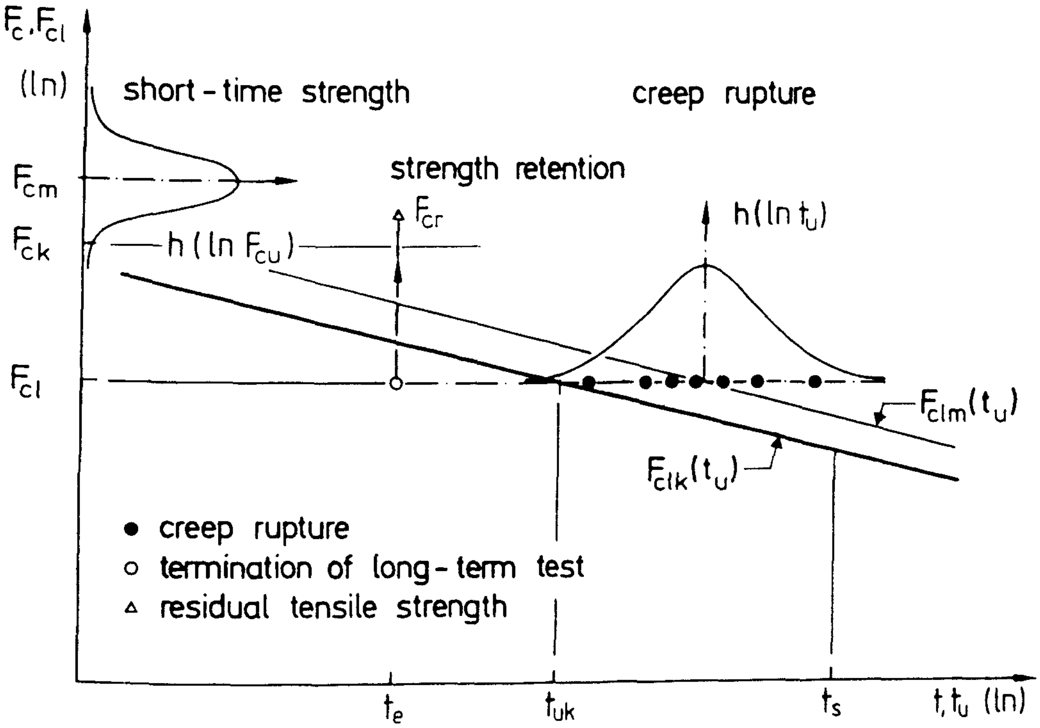

Fig. 4.14: Creep Rupture and Strength Retention

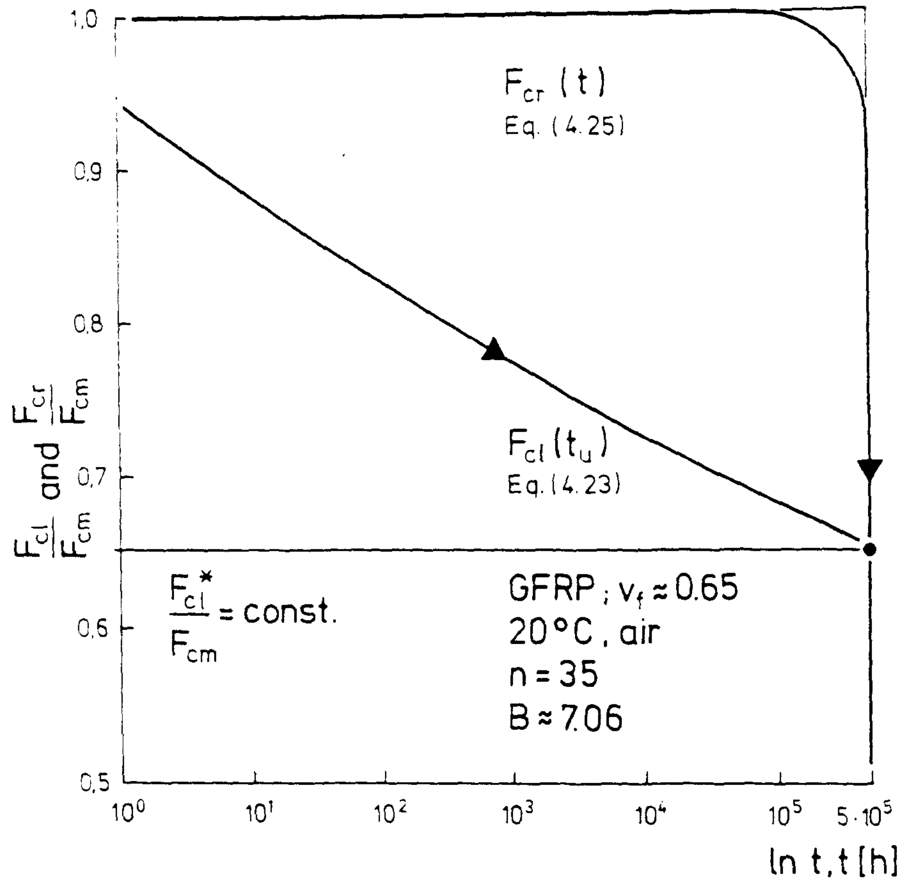

Fig. 4.15: Theoretical Creep Rupture Line

strain mirrors the accumulation of damage which is caused by the increase of delaminations and fiber fractures (Fig. 4.13).

As shown schematically in Fig. 4.14 the endurance time t_u will scatter strongly. Large coefficients of variation v_{tu} of 50 to 100 % are reported in literature. Provided a sufficient number of creep rupture tests on distinctly different force levels F_{cli} were performed, statistical evaluation will render the endurance lines with a certain confidence (i.e. survival probability). The mean value of the endurance $F_{clm}(t_u)$ with a survival probability of 50 % and the usual characteristic endurance $F_{clk}(t_u)$ with e.g. a survival probability of 95 % can be determined. The relevant lines are drawn in Fig. 4.14. Comparison can be drawn with the short-time characteristic strength F_{ck}. The characteristic force $F_{clk}(t_s)$ at the end of service life is important for the stipulation of the admissible prestress. For the prediction of endurance, extensive testing is necessary.

For the evaluation of the tests and, expecially, for the prediction of the endurance for the duration of service life, theoretical models are valuable. By applications of the fracture mechanics concept for the time- and stress-dependent growth of damage, the following equation for the endurance is given in [4.7]:

$$\frac{F_{cl}}{F_{cu}} = (Bt_u)^{-\frac{1}{n}} = \left(B\,\frac{t_u}{t_0}\right)^{-\frac{1}{n}} \tag{4.23}$$

or with ln the natural logarithm:

$$\ln\left(\frac{F_{cl}}{F_{cu}}\right) = -\frac{1}{n}\ln B - \frac{1}{n}\ln\left(\frac{t_u}{t_0}\right) \tag{4.24}$$

with t_0 = 1 h, t_u in hours; B is a flaw size parameter relevant for the described material and element; n is a material parameter. Both, B and n, must be derived on basis of tests. Eq.(4.24) represents a straight line in a double-ln plot. Fig. 4.15 shows the evaluation of Eq.(4.24) for a set of material parameters B and n, which were derived from tests with GFRP bars [4.6]. The creep rupture force F_{cl} is related to the mean tensile short-time strength F_{cm}. The example shows that a permanent force of 0.65 F_{cm} would lead to failure after about $5 \cdot 10^5$ hours of loading.

Fig. 4.16 shows test results for GFRP bars, tested in air of 20°C/65 % r.h. The mean curves and the range of scatter of test results are drawn [4.4]. In Fig. 4.17 test results of ARAPREE flat strips subjected to alkaline solution in order to simulate the effect of concrete pore water are depicted [4.12]. Both the mean creep rupture line and the one with a survival probability of 95 % were evaluated and drawn according to Eq.(4.23). AFRP are less sensitive to alkaline solutions than GFRP. CFRP are not significantly affected at all by the latter.

4.3.2.2 Strength retention

Creep rupture entails a cumulative damage in course of time, commencing some time prior to final failure. For the ultimate limit state design the original tensile strength of the FRP be available during service life t_s without any significant loss.

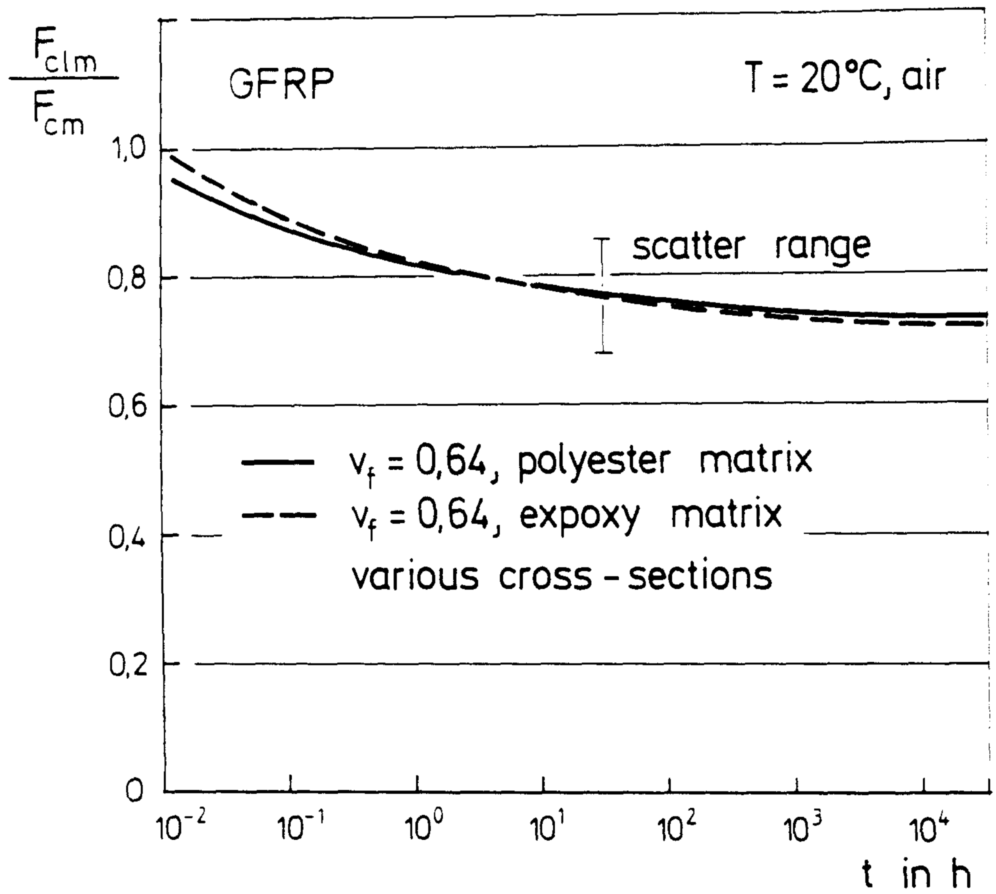

Fig. 4.16: Creep Rupture of GFRP (Various Authors)

If the sustained loading under F_{cl} is removed - prior to creep rupture - at the time t_e, the residual tensile strength F_{cr} can be measured. An analytical expression for the strength retention was derived in [4.7] on basis of Eq.(4.23) and with a suitable damage criterion:

$$\frac{F_{cr}(t_e)}{F_{ck}} = \left\{1 - \frac{t_e}{t_u}\left[1 - \left(\frac{F_{cl}(t_u)}{F_{cu}}\right)^{n-2}\right]\right\}^{\frac{1}{n-2}} \tag{4.25}$$

This formula has been evaluated in Fig. 4.15 for the given example. Damage develops rapidly if $t_e > 10^5$ hours. At $t_e = t_u = 5 \cdot 10^5$ hours strength retention has vanished.

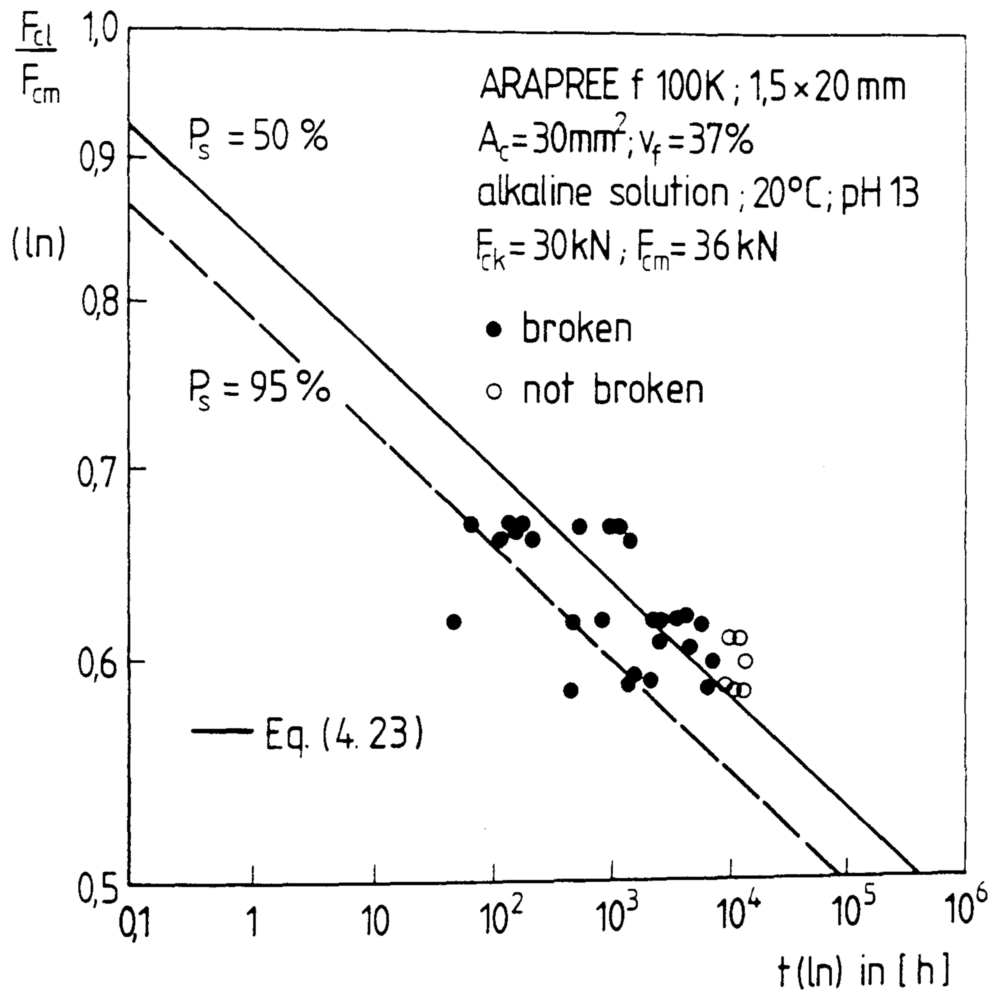

Fig. 4.17: Creep Rupture of ARAPREE in Alkaline Solution

The permissible permanent prestress of a FRP element has to be chosen in such a way that during service life an adequate residual strength is available. A reasonable requirement for this would be:

$$\frac{F_{cr}(t_e)}{F_{ck}} = \beta \geq 0,95 \tag{4.26}$$

In practice the permanent force F_{cl} will be in the range of 0,5 to 0,6 F_{ck}. For a stipulated service life t_s the relevant endurance time t_u can be expressed:

$$t_u \geq t_s \frac{1 - \left(\frac{F_{cl}}{F_{ck}}\right)^{n-2}}{1 - \left(\frac{F_{cr}}{F_{ck}}\right)^{n-2}} \approx t_s \frac{1}{1 - \left(\frac{F_{cr}}{F_{ck}}\right)^{n-2}} \tag{4.27}$$

The Eq.(4.22) to (4.27) are deterministic formulations. For the analysis of reliability the scatter of F_{cl}, F_{cr}, and t_u must be taken into account. In Fig. 4.18 the results of strength retention tests of ARAPREE strips after sustained loading are shown [4.9].

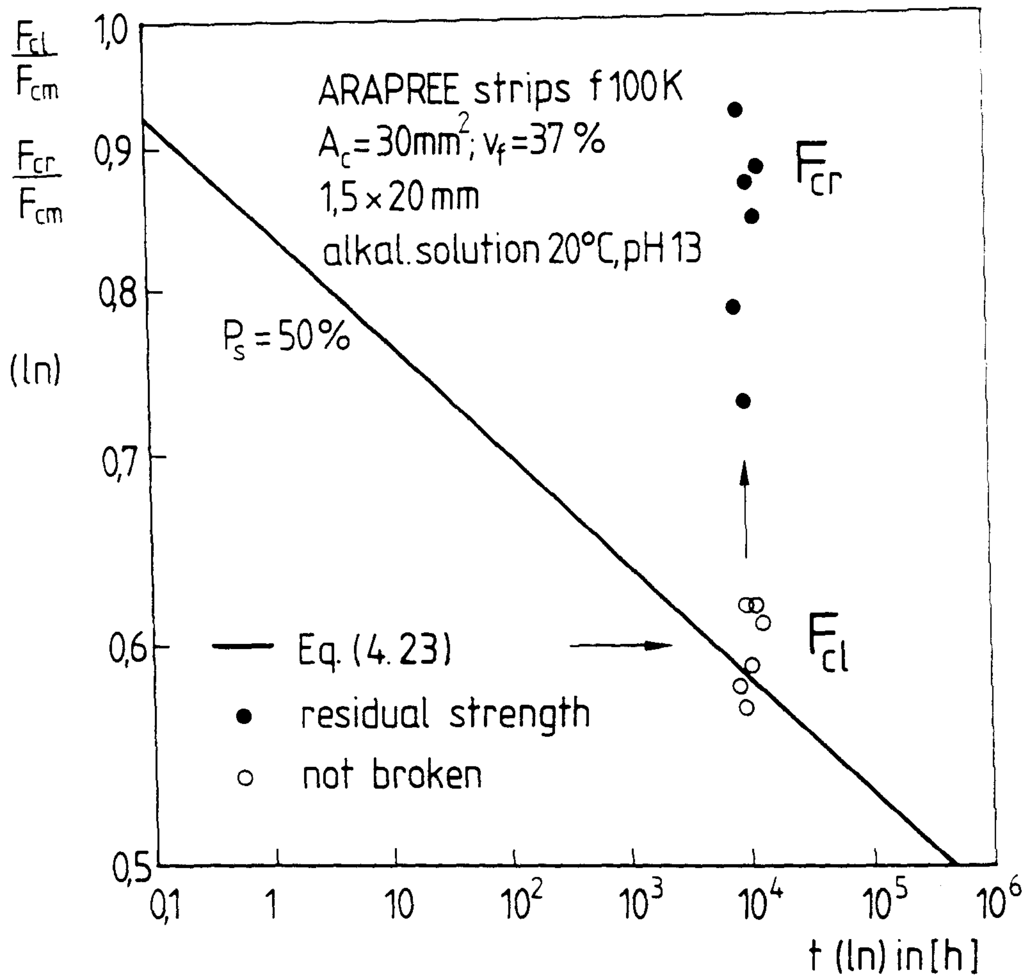

Fig. 4.18: Strength Retention of ARAPREE After Long-term Loading in Alkaline Solution

4.3.3 Influence of Environment on Creep Rupture Strength and Strength Retention

Environment encompasses, in the sense dealt with here, a plurality of influences. The influence of UV-radiation, sec. 4.2.6, can be precluded. The influence of temperature changes during regular service is rather unimportant, sec. 4.2.4.

The uptake of moisture reduces the short-term tensile strength of FRP only a little. It can be assumed that it will also reduce the creep rupture strength in the same magnitude.

The FRP dealt with here will not be damaged by ions from acidic solutions, such as chlorides. More important is the influence of alkaline solutions with pH 12,5 and higher: fresh concrete and the pore solution of hardened concrete. As the alkaline solution penetrates through the matrix to the fibers, it will adversely affect both the short-term and the long-term strength of glass and aramid fibers. This effect is of a stress corrosion type. Tests show that E-glass fibers are more severely attacked than S-glass fibers. If the matrix consists of epoxy resin, attack is diminished in comparison to a polyester matrix. Inhibitors, added to the matrix, will improve the long-term strength [4.8]. Though research shows promising ways to increase the long-term strength of GFRP, the latter have presently to be protected from contact with high alkaline solution.

Aramid fibers in epoxy matrix are less affected by high alkaline solution. Extensive tests have been performed to assess the creep rupture and strength retention of ARAPREE in cementitious solutions [4.9]. It was shown that by raising the temperature of the solution from 20°C to 60°C the prediction of behaviour at 20°C can be extrapolated for long duration (time factor 100; i.e. two decades). By testing the FRP-element in grout or cementitious solution the weakening effect of moisture is simultaneously incorporated.

CFRP are the least sensitive FRP materials to any kind of environmental influence.

4.3.4 Characteristic Long-Term Strength

4.3.4.1 Necessary test work

On basis of short-term static tensile tests the characteristic short-term strength F_{ck} has been determined, sec. 4.2.8. Creep rupture behaviour must be investigated on at least three distinctly different force levels F_{cli}, e.g.: 0,8; 0,7; and 0,6 F_{ck}; Fig. 4.14. The force F_{cli} is maintained constant until break occurs, the fracture times t_{ui} are being recorded. If the FRP element is to be used in practice in a detrimental environment then this has also to be considered in the tests, e.g.: cementitious, high alkaline solution in contact with the specimen on its free length. The range of endurance times t_u should cover up to 10^4 hours. Experience shows that at least 10 to 15 results t_{ui} per force level are necessary. It has to be pointed out that both weakening effects, moisture and alkaline attack are inseperably included in the test results.

4.3.4.2 Statistical evaluation

Characteristic endurance line of creep rupture

The endurance times t_{ui} of the specific force level F_{cli} exhibit considerable scatter. For the establishment of the mean and characteristic endurance lines, $F_{clm}(t_u)$ and $F_{clk}(t_u)$, $F_{clm}(t_u)$ is combined with a survival probability $P_s(t_u)$ of 50 %; $F_{clk}(t_u)$ with one of 95 % or 90 % survival probability.

Statistical evaluation requires the decision of a suitable probability density fuction $h(t_{ui})$ (e.g. Gaussian, Weibull or other types). Many evaluations show that the so-called inverse sine $\sqrt{P_s}$ transformation is a very simple and powerful tool for the statistical evaluation. To present details on the relevant numerical procedure is beyond the scope of this report. The interested reader is refered to the literature [4.10]. The result of the evaluation are characteristic endurance times t_{uk} on the chosen force levels F_{cli} in the F_{cl}-t double ln-plot (s. Fig. 4.14). The values t_{uk} can then be approximated using the Eq.(4.23) with the least square method. This procedure then leads to the forecast of the endurance line $F_{clk}(t_u)$ into the region of the service life span t_s. This is schematically shown by Fig. 4.14. The charakteristic endurance line can be expressed using Eq.(4.23):

$$F_{clk}(t_{uk}) = F_{ck}\left(B_k\,\frac{t_{uk}}{t_0}\right)^{-\frac{1}{n_k}} \tag{4.28}$$

Certainly, also other formulations can be chosen [4.12].

Coefficient of variation of long-term strength

For the stipulation of the permissible force on basis of partial safety factors the coefficient of variation v_{cl} of F_{clk} must be known. The determination of the latter proves to be difficult. Hence, an approximative method for this will be presented in the sequel.

In Fig. 4.19 schematically the mean and the characteristic endurance line are shown. From the statistical evaluation the characteristic endurance time t_{uk} and its standard deviation have been found. The endurance t_{uk} can be expressed - assuming a ln-normal distribution - by the mean value t_{um} of the endurance:

$$t_{uk} = t_{um}\,(1 - k \cdot v_t) \qquad (4.29)$$

with v_t the COV of the endurance time and with k the factor of the t-distribution.

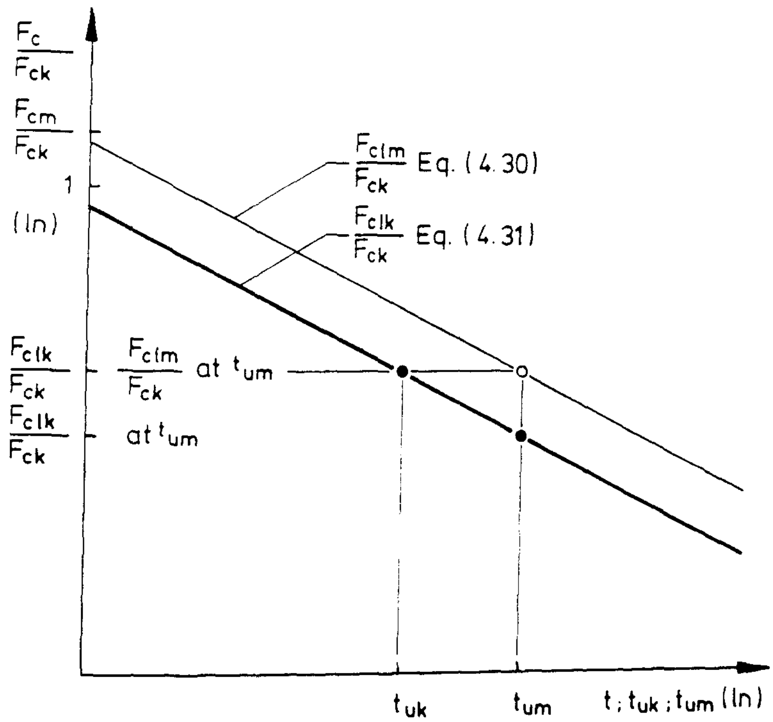

Fig. 4.19: Relation Between Mean and Characteristic F_{cl}-Line

If we assume, as shown by tests, that the lines $F_{clk}(t_{uk})$ and $F_{clm}(t_{um})$ are parallel to each other in double-ln-plot, both of them can be expressed with Eq.(4.23):

$$F_{clk}(t_{uk}) \approx F_{ck}\left(B_k\,\frac{t_{uk}}{t_o}\right)^{-\frac{1}{n}} \qquad (4.30)$$

and

$$F_{clm}(t_{um}) \approx F_{cm} \left[B_m \frac{t_{um}}{t_0} \right]^{-\frac{1}{n}} \tag{4.31}$$

The forces F_{clk} and F_{clm} are related according to Eq.(4.32):

$$F_{clk} = F_{clm} \; (1 - k \cdot v_{cl}) \tag{4.32}$$

with v_{cl} the unknown COV of F_{cl}. Because of

$$F_{clk}(t_{uk}) = F_{clm}(t_{um})$$

we obtain a relation between the factors B from Eq.(4.29), (4.30) and (4.31):

$$B_m = B_k \; (1 - k \; v_t) \tag{4.33}$$

If Eq.(4.32) and (4.33) are introduced into Eq.(4.30)and (4.31), the COV of the long-term strength v_{cl} can be deduced from the known COV of the endurance time v_t:

$$v_{cl} = \frac{1 - (1 - k \cdot v_t)^{\frac{1}{n}}}{k} \tag{4.34}$$

With this transformation of the COV the influence of the variability of the endurance times t_u on the variability of the long-term strength can be investigated. This is shown by Fig. 4.20. Eq.(4.34) delivers real solutions only between $0 \le v_t \le 1/k$; $1/k = 0{,}608$. Tests show that the COV of the short-term tensile strength v_c is in the range of 1.5 to 3.0 %. Hence, it must be expected that COV v_{cl} will exceed this low value. The curves of Fig. 4.20 - e.g. for two practical values of n - show the exponential increase of v_{cl} if v_t increases. Values of the COV v_t of 30 to 60 % were reported in the literature.

The described approximative transformation is not yet verified by experiments. Research is strongly needed.

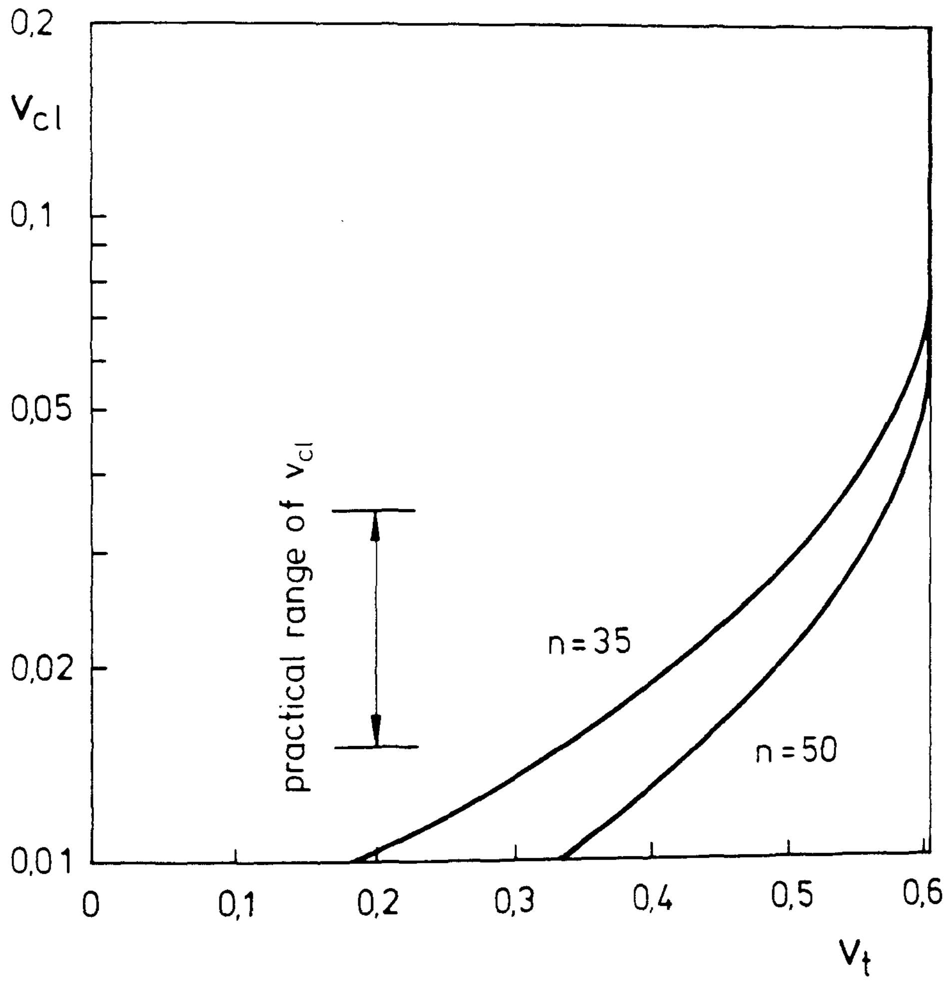

Fig. 4.20: Relation Between the COV v_{cl} and v_t

Strength retention

In the practical application the necessary duration of service life t_s is being a priori stipulated, e.g. $0{,}5 \cdot 10^6 \approx 57$ years. At the end of t_s adequate strength retention must be available, e.g. $F_{crk}/F_{ck} \approx 0{,}95$. Hence, the characteristic action S_{clk} must be less than $F_{clk}(t_s)$. An example may elucidate the evaluation. Thereby, the data of Fig. 4.15 are used. For $t_s = 0{,}5 \cdot 10^5$ hrs and $F_{crk}/F_{ck} \approx 0{,}95$ we obtain with Eq.(4.27).

$$t_{uk} = t_s \frac{1}{1-(0{,}95)^{n_k - 2}} \approx 1{,}226\ t_s = 0{,}613 \cdot 10^5 \text{ hrs}$$

and with Eq.(4.13)

$$F_{clk}(t_{uk}) \approx 0{,}646 \cdot F_{ck}$$

Thus, if a constant action S_{clk} is assumed to act, then at $t_s = 0.5 \cdot 10^5$ hrs the FRP element will still survive and have a strength retention of 0,95. Deliberations of this kind may serve as basis for the development of the design resistance.

4.3.5 Relaxation

For the estimation of the loss of prestress in course of time the stress relaxation of the tensile element must be known. The relaxation behaviour of the FRP elements treated here differs widely. The polymer matrix resins are visco-elastic materials, thus exhibiting relaxation. Glass fibers and carbon fibers show practically no relaxation. In contrast to these fibers, aramid fibers exhibit relaxation losses which increase with the decrease of the axial Young's modulus.

Of great influence on the magnitude of the relaxation loss is the environment the stressed FRP element is subjected to. An increase of temperature activates the relaxation, especially of the stresses imparted to the matrix. Hence, the relaxation losses increase the more the lower the fiber volume v_f.

In Fig. 4.21 the relaxation losses of GFRP bars (Polystal) and AFRP strips (ARAPREE) are depicted, with the specimens being stored in air of 20°C and 65 % r.h. during the tests. Duration of tests was about 1000 to 3000 hours. For the sake of comparison the mean relaxation losses of a high-strength prestressing steel wire (cold drawn, stabilized, low relaxation type) are included [4.9, 4.13 to 4.15]. For initial stresses $\sigma_i \leq 0{,}6\ f_{clk}$ the loss of stress for FRP is independent on the initial stress. The relaxation loss of the GFRP elements is only slightly higher than of prestressing steel wire. In contrast to this, the relaxation loss of the ARAPREE elements (Twaron HM fibers) is considerably higher.

If the FRP element is to be used for the pre-tensioning of concrete members or if it is embedded in cementitious grout, its relaxation in the alkaline environment of moist, non-carbonated concrete must be known. In Fig. 4.22 the relaxation of AFRP rods, ø 8 mm (Twaron) and of CFRP rods, ø 8 mm is depicted [4.16]. During the tests the bars were subjected to a high-alkaline solution of pH 13 which was heated to 60°C. Such severe test conditions are

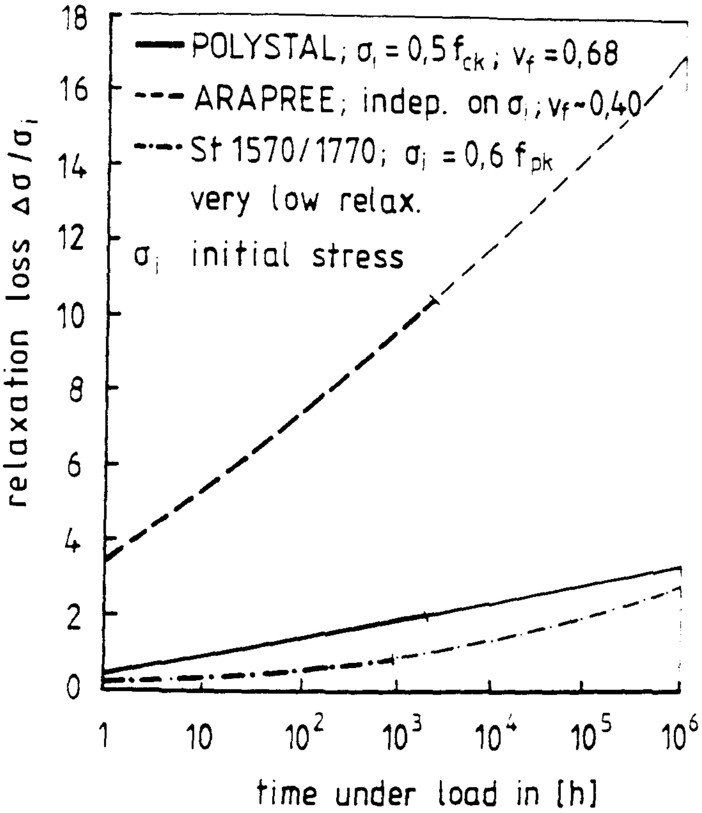

Fig. 4.21: Relaxation of Various FRP

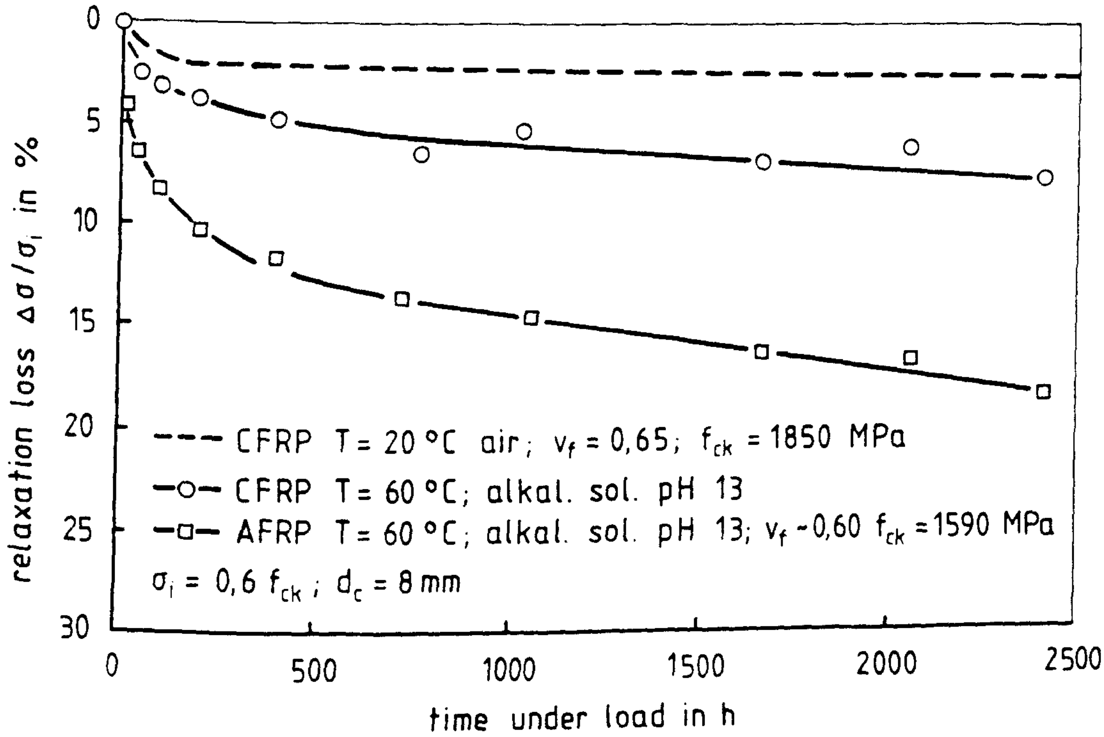

Fig. 4.22: Relaxation of CFRP and AFRP Rods

often used to accelerate the relaxation losses for the forecast of the long-term losses. As one might expect CFRP is less affected than AFRP under this condition. For comparison also the behaviour of the CFRP rods stared in air 20°C/65 % r.h. is shown.

In Fig. 4.23 test results for CFRP seven wire strands and for prestressing steel strands, both having a nominal diameter of 12,5 mm, are shown [4.17]. The strands were stressed to 80 % of their characteristic breaking force. Tests were performed in air 20°C/65 % r.h.. In [4.17] it also shown that a short-time heating to 60°C for about 10 hours did not increase the relaxation of the CFRP strand. In contrast to this the relaxation of the highly stressed prestressing steel strand increased strongly due to this procedure.

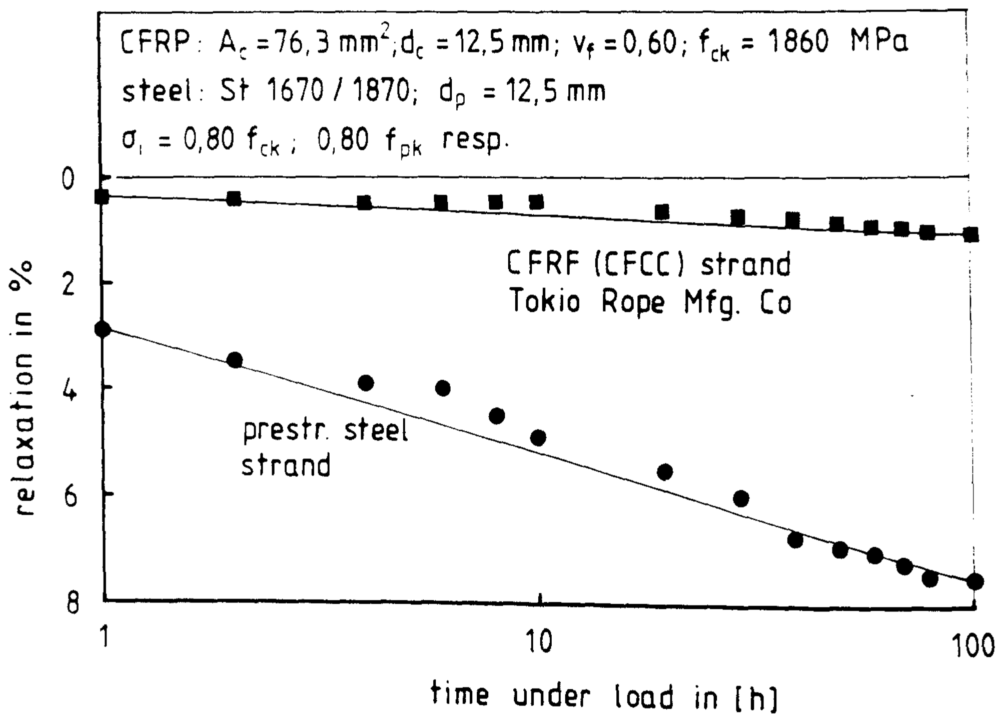

Fig. 4.23: Relaxation of CFRP Strands and of Prestressing Steel Strands

Although the experimental basis for the forecast of the relaxation losses over several decades is rather small, Fig. 4.21 shows that they seem to increase with logarithm of the time under load. The high relaxation losses of especially AFRP elements are for the design of prestressed concrete members of negligible influence when calculating the total loss of prestress due to shrinkage, creep and relaxation. Shrinkage and creep of concrete are transformed into the loss of steel stress with the ratio of the moduli of elasticity $E_p/E_{cr} \approx 5,5$ to $6,5$ (E_p, prestressing steel; E_{cr}, concrete). For AFRP this ratio is in the range of

$$\frac{E_c}{E_{cr}} \approx 3 \text{ to } 3,5.$$

Hence, shrinkage and creep induced losses of prestress are about half as great. Consequently the higher relaxation of AFRP is compensated.

4.4 Mechanical Behaviour under Dynamic Loading

Especially when using FRP elements for the prestressing of concrete bridges their fatigue behaviour must be known. Fatigue behaviour is usually assessed in constant stress amplitude cyclic tension tests with a constant upper stress σ_{cu}. The latter corresponds to the admissible prestressing stress which is for FRP in the range of 0,45 to 0,60 f_{ck}. By varying the stress range $\Delta\sigma_c = \sigma_{cu} - \sigma_{cl}$ the S-N-curve can be established as function of the load cycles until failure. For the fatigue testing it is very important to have a laboratory anchorage which does not reduce the fatigue strength of the FRP-material, e.g. by fretting.

Information on tests which follow the above-mentioned requirements is rather scarce. In Fig. 4.24 several FRP materials are compared with high-strength prestressing steel wire (GFRP [4.18], AFRP [4.19], CFRP [4.20] and prestressing steel [4.21]). The fatigue strength of the investigated AFRP and CFRP elements exceeds prestressing steel. It should be remarked that the CFRP specimens of Fig. 4.24 did not fail by fatigue. The tests were terminated prior to failure. The fatigue strength of the GFRP elements - if polyesther resin matrix is used - is rather low. With an epoxy matrix fatigue behaviour can be improved as Fig. 4.25 shows [4.8].

In Fig. 4.26 fatigue rest results for CFRP rods of 8 mm diameter are depicted [4.16]. These tests were performed with a constant stress ratio $R = \sigma_{cl}/\sigma_{cu} = 0,1$. For 10^7 load cycles the fatigue strength for $\sigma_{cu}/f_{ck} \approx 0,57$ is with $\Delta\sigma_c \approx 1000$ MPa very high. It surpasses the fatigue strength of high-strength prestressing wire and strands by far.

Lately also test results for CFRP severe wire strands with a nominal diameter of 12.5 mm have been reported [4.17]. In Fig. 4.27 the results are plot

Fig. 4.24: S-N Lines of Several FRP and of Prestessing Steel

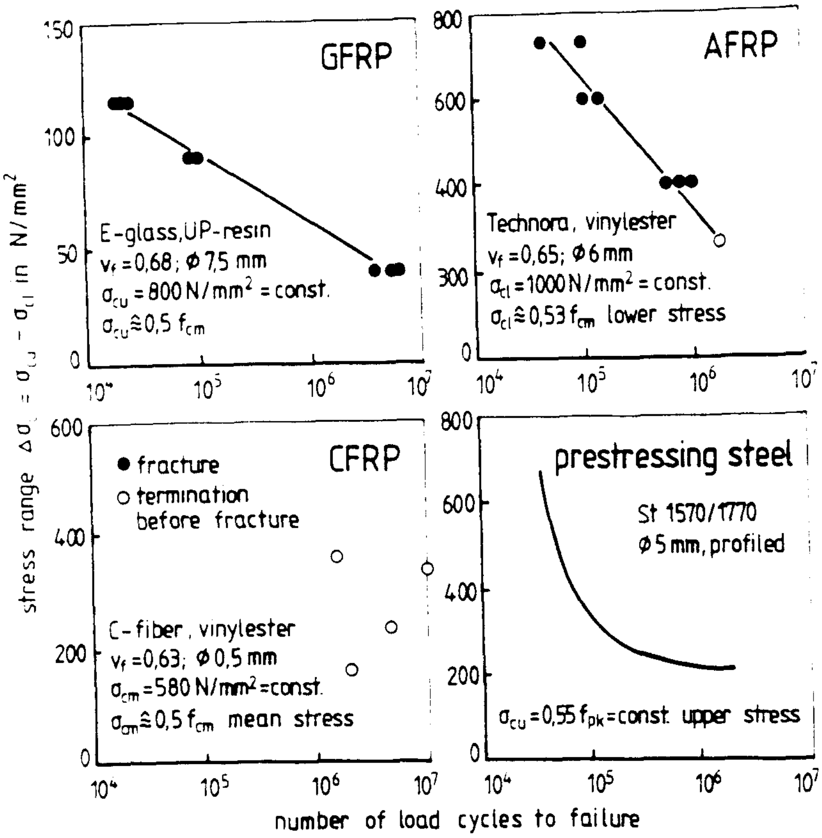

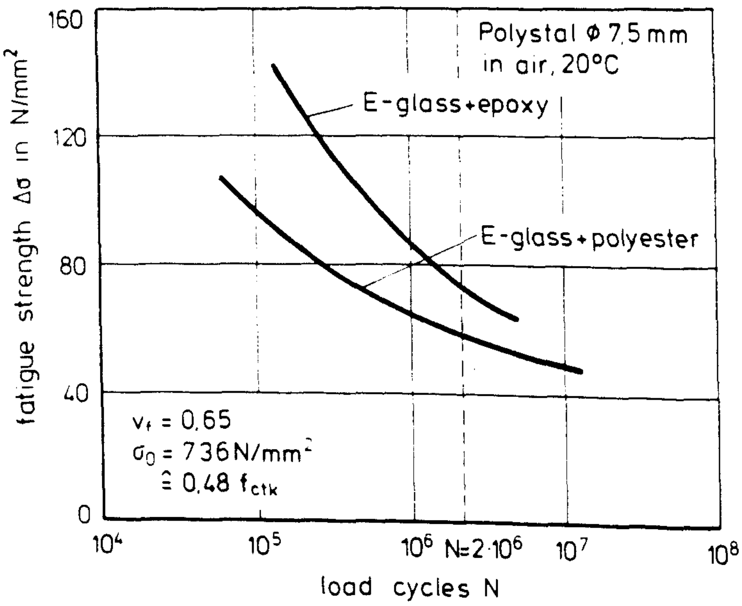

Fatigue behaviour of Polystal-bars

Fig. 4.25: Fatigue Behviour of Polystal Bars Dependent on Matrix Resin

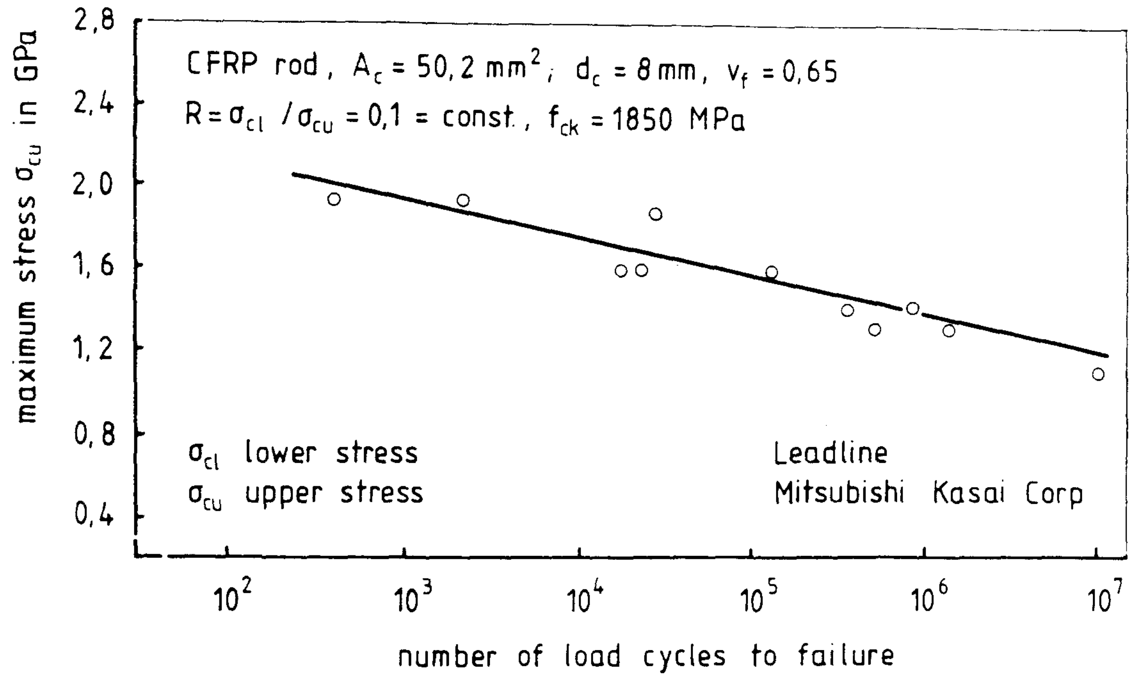

Fig. 4.26: S-N Line of CFRP Rods (Leadline)

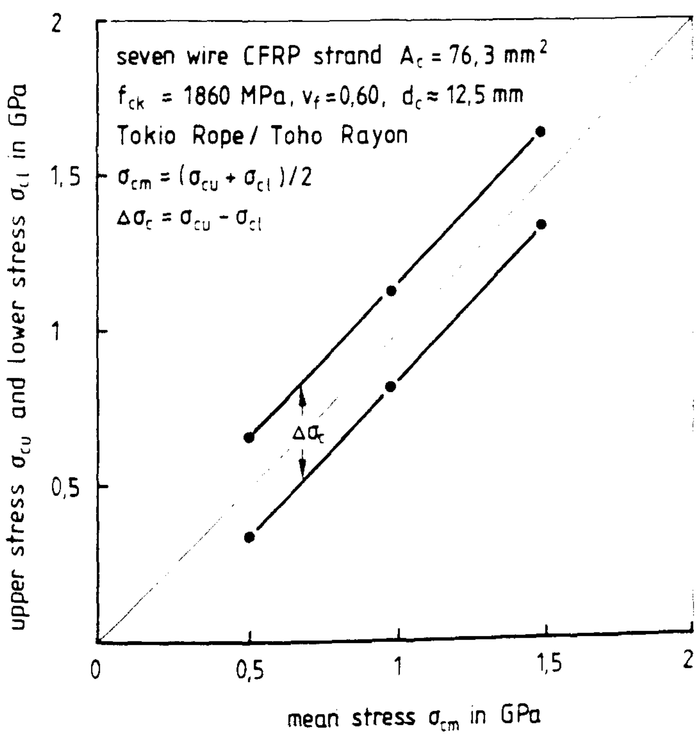

Fig. 4.27: Smith Diagram of Fatigue Strength of CFRP Strand (Tokio Rope)

ted in a Smith diagram. For an upper stress of $\sigma_{cu} \approx 1150$ MPa $\approx 0{,}62\ f_{ck}$ a stress range of $\Delta\sigma_c = 310$ MPa was endured for $2 \cdot 10^6$ load cycles. Prestressing steel strand St 1570/1770 exhibits under such condition a fatigue stress range of about $\Delta\sigma_p \approx 200$ MPa. It is interesting to note that the stress range is almost independent on the mean stress σ_m.

4.5 Literature

[4.1]: Chawla, K.K.: Composite Materials. Science and Engineering. Springer-Verlag, New York, 1987.

[4.2]: Rüegg, Ch.: Kohlenfaser- und Aramidfaserkunststoffe für Kardanwellen. Verarbeiten und Anwenden kohlenfaserverstärkter Kunststoffe. VDI-Verlag, Düsseldorf, 1981.

[4.3]: Niederstadt, G.: Einfluß der Betriebsbedingungen auf das Festigkeitsverhalten von CFK. Leichtbau mit kohlenstoffaserverstärkten Kunststoffen. Band 167, Kontakt & Studium Werkstoffe, Expert Verlag, Sindelfingen, 1985.

[4.4]: Rehm, G.; Franke, L.: Kunstharzgebundene Glasfaserstäbe als Bewehrung im Betonbau. Deutscher Ausschuß für Stahlbeton, Heft 304, 1979.

[4.5]: Helmer, T.; Wanner, A.; Kromp, K.: Prüfmethoden für faserverstärkte Keramiken. Prüfen neuer Werkstoffe, Prüfmethoden - Anwendung und Aussagefähigkeit. DVM-Tag 1990, Bauteil '90, S. 297 - 312.

[4.6]: Rehm, G.; Schlottke, B.: Übertragbarkeit von Werkstoffkennwerten bei Glasfaser-Harz-Verbundstäben. Mitt. des Inst. für Werkstoffe, Universität Stuttgart 1987/3.

[4.7]: Franke, L.: Schadensakkumulation und Restfestigkeit im Licht der Bruchmechanik. Festschrift G. Rehm, Verlag W. Ernst u. Sohn, Berlin.

[4.8]: Franke, L.; Wolff, R.: Fibre Glass Tendons for Prestressed Concrete Bridges. IABSE-Congress, Helsinki, June 1988, pp. 51/56.

[4.9]: den Uijl, J.A.: Mechanical Properties of Arapree. Part 4: Creep and Stress-rupture. Report 25-87-31, TU Delft, 1991.

[4.10]: Dengel, D.: Empfehlungen für die statische Abschätzung des Zeit- und Dauerfestigkeitsverhaltens von Stahl. Mat.-wiss. u. Werkstofftech. 20 (1989), pp. 73/81.

[4.11]: Niederstadt, G.: Kriterien und Beispiele für die Wahl von Verbundwerkstoffen mit Fasern hoher spezifischer Eigenschaften. Kunststofftechnik, Kohlenstoff- und aramidfaserverstärkte Kunststoffe. VDI-Verlag, Düsseldorf, 1977.

[4.12] Chiao, T.T.; Wells, J.E.; Moore, R.L.; Hamstad, M.A.: Stress-Rupture Behavior of Strands of an Organic Fiber/Epoxy Matrix. 3rd Conf. on Composite Materials: Testing and Design, ASTM STP 546, 1974, pp. 209/224.

[4.13] Gerritse, A.; Maatjes, E.; Schürhoff, H.J.: Prestressed Concrete Structures with High-Strength Fibres. IABSE Report Vol. 55, Zürich, 1987, pp. 425/432.

[4.14] Gerritse, A.; Schürhoff, H.J.; Maatjes, E.: Prestressed Concrete Structures with Arapree; Relaxation. IABSE-Symp.: Concrete Structures for the Future, Versailles, 1987.

[4.15] Waaser, E.; Wolff, R.: Ein neuer Werkstoff für Spannbeton. HLV-Hochleistungs-Verbundstab aus Glasfasern. beton 36, 1986, H.7, pp. 245/250.

[4.16] Leadline Product Information on Carbon Fiber Tendons/Bars by Mitsubishi Kasai Corp., 1991.

[4.17] Zoch, P.; Kimura, H.; Iwasaki, T.; Heym, M.: Zugelemente aus kohlenstofffaserarmiertem Kunststoff, eine neue Klasse von Vorspannmaterialien. Forschungskolloquium am Institut für werkstoff im Bauwesen, Universität Stuttgart, Nov. 1991.

[4.18] Franke, L.; Overbeck, E.: Dauerschwingverhalten von Glasfaserverbundstäben im anwendungsorientierten Zugschwellbereich. Bautechnik 66, 1989, H.3, pp. 90/92.

[4.19] Kakihara, R.; Kamiyoshi, M.; Kumagi, S.; Noritake, K.: A New Aramid Rod for the Reinforcement of Prestressed Concrete Structures. ASCE Spec. Conf.: Advanced Composites Materials in Civil Engineering Structures, Las Vegas, 1991, pp. 132/142.

[4.20] Walton, J.M.; Yeung, Y.T.C.: The Fatigue Performance of Structural Strands of Pultruded Composite Rods. Journal of the Institute of Mechanical Engineers, London, C 286/86, 1986, pp. 315/320.

[4.21] Nürnberger, U.: Dauerschwingverhalten von Spannstählen. Bauingenieur 56, 1981, pp. 311/319.

5. CORROSION RESISTANCE OF FRP

5.1 Practical Relevance

One of the main reasons of the search for alternatives for reinforcing and prestressing steel is the danger of corrosion for normal carbon steel under conditions like low alkalinity of the concrete due to carbonization and chloride contamination of the concrete cover. But it is also well known, that the durability of some polymers and fibers, especially in alkaline environments is insufficient.

If FRP are to overcome the corrosion susceptibility of steel in aggressive environments they have to ensure, that they can withstand sufficiently such conditions during the service life of the concrete member.

5.2 Relevant Environments

The basic environment for the reinforcing and prestressing with FRP or steel elements is the concrete itself. For FRP elements is - which respect to eventual corrosion - the composition of the pore water solution of the concrete essential. The composition depends on the type of the cement and varies especially in the amount of alkalies. Usually the pore solution consists of a saturated $Ca(OH)_2$ solution with 4 - 10 g/l Na^+ and K^+ (expressed as Na^+-equivalent) ions.

The pH-value of an uncarbonated concrete is about 13. Due to carbonization the content of $Ca(OH)_2$ and of free Na^+ and K^+ decreases considerably. Since the carbonization process cannot be predicted accurately, the relevant environment for the investigation of the corrosion of FRP elements should be either an uncarbonated concrete or an equivalent solution, because this environment causes the strongest chemical attack to FRP.

When examining the durability of FRPs it is difficult to embed the specimens in concrete and to subsequently recover them from the concrete for testing without damage. Therefore artifical solutions should be used. For these solutions it is very important to use not only a saturated $Ca(OH)_2$ solution, but also a solution containing alkali ions. Because of the different ion diameter and the different electrical loading, the diffusion velocity of Ca^{++} is lower than that of Na^+ and K^+. As the chemicals have to diffuse through the matrix resin before they can attack the fibers, their diffusion velocity through the resin is of great importance. For this reason a test solution consisting of saturated $Ca(OH)_2$ + 0,4 n KOH is recommended.

Chloride in concrete do not attack any of the FRP elements treated here. Therefore chloride containing solutions do not have any value in the tests. Other chemicals like acids and solvents could be important for the durability of the tensile elements if they come into contact with them. Because concrete is a porous material this could happen, e.g. in case of storage facilities. Therefore the chemical resistance of FRP should be tested with all chemicals relevant to a specific application.

5.3 Types and Mechanisms of Corrosion

5.3.1 Corrosion of Aramid Fibers

Strength and stiffness of aramid fibers depend on the chemical structure of the polymer. The polymer is built up out of hundreds of long and stiff molecular chains, which are interconnected by hydrogen bonds. A part of these chains is shown in Fig. 2.2.

Aramids are affected by two different chemical processes. One process is the degradation of hydrogen bridges. If water molecules diffuse into the polymer, the hydrogen bonds are resolved and the bond between the chains is reduced. As result of this the strength decreases. But this process is reversible if the FRP element is dried.

A real corrosion process occurs in the presence of alkaline solutions. KOH solutions for instance hydrolize the linkages between the C and the N atoms and the long chains are cut.

Since the strength of the aramid fibers depends on the length of the molecules, a decrease of the length of the molecular chain results in a lower strength. This process is irreversible.

5.3.2 Corrosion of Carbon Fibers

Because of their chemical structure carbon fibers are inert against nearly all chemicals. They do not corrode in any of the environments concrete structures will normally be subjected to.

5.3.3 Corrosion of Glass Fibers

The corrosion process of glass fibers in strong alkaline solutions has not yet been precisely examined. Probably the complex silicate ions dissolve as a function of the pH value. Thereby the silicate network is decomposed, while in case of an acid environment only single ions are exchanged against H^+ ions.

The reaction products of the alkaline corrosion process form a layer upon the fiber surface which becomes thicker and thicker. This layer is normally not tight against alkali ions, so that the degradation process continues with time. It was found out, that the alkaline corrosion resistance of different kinds of glass fibers mainly depends on the content of multivalent metal oxides. These metal oxides form a layer on the fiber surface. If unsoluable Ca compounds are available, these compounds are integrated in the surface layer and condenses it to an extent, that it becomes tight against alkali ions.

The alkali resistance of glass fibers can be enhanced by the addition of ZrO_2 and TiO_2.

5.3.4 Rate of Corrosion

The velocity of corrosion is dominated by two processes. The first process is the diffusion, which is determined by the time t, the absolute temperature T, the gradient of concentration c, the length of the diffusion path x, diffusion coefficient D and the cross-sectional area of diffusion q. The equation for this process is:

$$\frac{\Delta m}{\Delta t} = D \frac{dc}{dx} \tag{5.1}$$

with the diffusion coefficient

$$D = D_0 \exp\left(- \frac{E}{RT}\right) \tag{5.2}$$

wherein

m .... mass flux of diffused material
E .... activation energy
R .... universal gas constant
D_0 ... basic diffusion coefficient

If corroding substances have reached the fibers, the velocity of the chemical degredation process v is determining the residual strength r.

$$f(v) = r \tag{5.3}$$

Chemical reactions like hydrolysis of the C-N link in case of the aramids or the dissolution of complex silicate ions in case of glass follow the Arrhenius equation:

$$v = A \exp\left(- \frac{E}{RT}\right) \tag{5.4}$$

$$\frac{d(1-r)}{dt} = K \exp\left(- \frac{E}{RT}\right) \tag{5.5}$$

with K as a constant, which can be determined by variation of the temperature of the test. Thereby it is possible to accelerate the corrosion by elevated temperature and to be able to predict the long-term behaviour by means of tests taking only some months.

5.4 Corrosive Effects on Strength

One has to distinguish between the temporary and permanent reduction of strength. In the case of aramid fiber composites water saturation leads to a temporary reduction of strength of 5 to 10 % and a reduction of tensile Young's modulus of 5 % because of the degradation of H-bridges. This loss of strength is nearly fully reversible when the composite is dried.

In an alkaline solution, as described in sec. 5.2, the residual strength of an aramid/epoxy composite is 95 % of the initial strength at a temperature of 20 °C after 100 years.

Generally valid data for the development of residual strength of glass fiber composites cannot be presented, because the influence of type of glass and type of resin is very important. Comparable tests between aramid/epoxy composites and E-glass/epoxy composites show a higher loss of strength in alkaline solutions for the glass fiber composites.

5.5 Protective Measures

The most important protective measure to increase the corrosion resistance of AFRP and GFRP is the choice of the matrix resin. Resins with a high diffusion resistance should be preferred.

An outer layer of resin without fibers prolongs the time of diffusion. Measures like coating with thermoplastics are not very effective, because their diffusion resistance against water and alkalies is low.

If the long-term corrosion resistance of a composite is too low, the alkalinity of the concrete can be reduced. One possibility is the choice of cements and concretes with a lower alkalinity. In case of post-tensioning with bonded tendons the use of resin mortars for the injection of the ducts may also be solution.

6. THERMAL, HYGROSCOPIC AND ELECTRICAL PROPERTIES OF FRP

6.1 Practical Relevance

FRP when applied as reinforcing and/or prestressing tensile elements for structural concrete or ties or ground anchors are subjected to thermal and hygroscopic influences. Some of the effects of temperature and moisture with respect to strength have already been discussed in sec. 4.2. Others, together with the electrical properties will treated be here.

6.2 Thermal Properties

6.2.1 Thermal Dilatation

As shown by Table 6.1 the components matrix and resin differ markedly with respect to their thermal expansion. The matrix resins behave isotropically, though differing dependent on their chemical composition. Glass fibers are also an isotropic material. Aramid and carbon fibers however are with respect to thermal dilatation orthotropic. These facts lead to several consequences.

From [6.1] the coefficient of axial thermal expansion of the composite can be described if the coefficients of the components are known:

$$\alpha_{cl} = \frac{\alpha_{ml}\ E_{ml}\ v_m + \alpha_{fl}\ E_{fl}\ v_f}{E_{ml}\ v_m + E_{fl}\ v_f} \tag{6.1}$$

and the one transverse to the fiber axis ($v_f > 0{,}3$) is:

$$\alpha_{ct} = (1 + v_m)\ \alpha_{mt}\ v_m + \alpha_{ft}\ v_f \tag{6.2}$$

As the resultant coefficients depend on the columes v_f, v_m, etc. their values will vary strongly. In Tab. 6.2 the calculated coefficients are presented for $v_f = 0.7$ and for $E_m = 4$ GPa. For the specific material they have to be determined experimentally.

Table 6.1: Coefficients of Thermal Expansion and Young's moduli of Resins and Fibers (Basic Information)

property	unit	epoxy resin	polyester resin	E-glass	S-glass	aramid HM	carbon HT
α_l	$10^{-6} \cdot K^{-1}$	40-60	60-80	5,3	4	-3,5	-0,5
α_t	$10^{-6} \cdot K^{-1}$	40-60	60-80	5,3	4	60	5,5
E_l	GPa	3-5	3-5	74	86	130	240
E_t	GPa	3-5	3-5	74	86	5,4	16

Table 6.2: Calculated Coefficients of Thermal Expansion of FRP for v_f = 0,7

property	unit	GFRP E	GFRP S	AFRP HM	CFRP HT
α_{cl}	$10^{-6} \cdot K^{-1}$	6,3	4,9	- 2,0	- 0,1
α_{ct}	$10^{-6} \cdot K^{-1}$	23,2	22,3	31,4	23,4

6.2.2 Thermal Stresses

The thermal and mechanical mismatch between the components fibers and matrix will lead to internal stresses in the FRP element if a change of temperature ΔT occurs. Although the difference $\Delta\alpha = \alpha_m - \alpha_f$ is very large, the resultant stresses in both components will remain rather small because of $E_m << E_f$ for an expected temperature difference $\Delta T \approx \pm 40$ K in concrete structures.

If the FRP element is embedded in concrete or grout the difference in the thermal and mechanical properties of FRP and concrete will lead to thermal restraint stresses if the concrete member as a whole experiences a temperature change ΔT. It can be shown that resultant axial and radial restraint stresses in the FRP element itself are not significant. However the radial thermal expansion of the FRP element may cause sizeable concrete tensile stresses if the cover is small. Although the problem can be treated analytically it is recommended to study it by tests. Relaxation will reduce the stresses in the matrix.

6.2.3 Combustability

FRP are combustible materials due to the polymeric resin. Thus, for such purposes where an adequate fire resistance of the structural element is required, protective measures are necessary (sufficient concrete cover, thermally insulating cover, etc.).

6.3 Hygroscopic Properties

6.3.1 Water Absorption

A fiber composite will absorb water when stored for a long time in moist environment (e.g. also in fresh and hardened concrete, etc.). This leads to an increase of weight per unit volume and to swelling. Both water absorption and swelling are reversible processes, vanishing upon drying.

The fibers behave differently with respect to water absorption. While glass and carbon fibers do not absorb water, aramid fibers will. Aramid fibers will attain, when stored in a climate of 20 °C/65 % r.h., an equilibrium moisture content of about 3 - 4 m.-%, or when stored under water about 8 m.-% (mass percent). Because absorption and desorption of FRP is mostly connected with the change of ambient temperature, it is often denoted as hydrothermal behaviour.

The greater portion of the water, absorbed in FRP, is stored within the macromolecular structure of the matrix resin. As the water molecules force the polymer chains apart, swelling of the FRP transverse to the fiber axis occurs. This leads to several consequences. The glass transition temperature and the strength of the FRP are lowered with increasing moisture content (max $\Delta_{mc} \approx 4$ to 8 %). Hygroscopic stresses arise.

6.3.2 Swelling and Hygroscopic Stresses

As for the thermal expansion, the swelling of FRP depends also on the volume fractions and mechanical properties of the components. Swelling is only significant in the direction transverse of the fiber axis. The transverse coefficient of swelling can be expressed for a CFRP in epoxy matrix with $v_f \approx 0{,}58$ at 20 °C dependent on the absorbed mass of water [6.2]:

$\alpha_{cts} \approx 5 \cdot 10^{-3}$/m.-%, and the swelling strain is then

$$\varepsilon_{cts} \approx \alpha_{cts} \cdot \Delta m$$

with Δm the mass gain in m.-% due to water absorption. Swelling in axial direction is practically nil.

Swelling will also entail internal hygroscopic stresses comparable with thermal stresses. They will be significally reduced by stress relaxation. The tightness of the matrix resin against ingress of water is an important property.

As mentioned the uptake of water reduces the tensile strength slightly. Upon drying the loss of strength is regained, s. sec. 4.2.5.

6.4 Electrical and Magnetic Properties

FRP cannot conduct electrical currents nor can they be electrically magnetized. This virtue may be of advantage for several practical applications, e.g. for antenna stays.

6.5 Literature

[6.1] Chawla, K.K.: Composite Materials Science and Engineering. Springer-Verlag, New York, 1987.

[6.2] Niederstädt, G.: Verbund- und Hybridwerkstoffe. Neue Methoden für Konstruktion und Fertigung. VDI BW 43-10-04, April 1990.

7. COMPARISON AND VALUATION OF FRP ELEMENTS

7.1 Foreword

The database of the FRP, given in Table 7.1, is incomplete and most of the long-term properties have been derived from short-term testing, although the materials have been applied already in projects. Nevertheless, the materials can be compared with each other.

Table 7.1: Survey of Manufacturers of FRP for Civil Engineering

manufacturer	country	fiber	matrix	brandname
Akzo	NL	A,C	EP	Arapree
Arisawa	J	A,C,G	EP	
Bayer AG	D	G	UP	Polystal
Bridson Composites	GB	A,C,G	EP,UP	Bri-ten
Cousin	F	G	UP	JONCS JT
IMCO	USA	G	UP	
Kuraray	J	PVA	EP	
Mitsubishi Kasei	J	C	EP	Leadline
Mitsui constr.	J	A	EP	Fibra
Polygon	USA	G	EP	
Pultrall	CAN	G	UP	Isorod
Sportex	D	G	EP	
Teijin	J	A	VE	AFRP rod
Tokyo rope	J	C	EP	CFCC

7.2 Matrix Resins

As can be derived from Table 7.1, the matrix resins have no considerable influence on the mechanical properties of FRP. But they contribute significantly to the durability of the composites, if the fibers are susceptible to a special environment. Even within one class of resins, e.g. the epoxy resins, there is a great difference in their diffusion resistance to various chemicals, as tests carried out by Akzo have shown.

The ranking in terms of protecting the fibers from corrosion is:

high protection ⟶ low protection
epoxies - vinylesters - unsaturated polyesters

Concerning the processing of the resins, the viscosity is of major importance. A low viscosity enables a high production speed, which reduces the cost price of the FRP. The order of costs including the raw material costs of the resins is:

high production costs ⟶ low production costs
epoxies - vinylesters - unsaturated polyesters

7.3 Mechanical Properties

The mechanical properties of the FRP are mainly determined by the fibers and the applied production technology.

The tensile strength related to the same fiber cross-section is slightly influenced by the type of fiber, except the PVA composite, which has a much lower strength. For the most part it is in the range between 2400 MPa and 3000 MPa.

But there is a distinct influence of the production technology with respect to arrangement of the fibers in the composite on the strength. Although the tensile strengths of the pure fibers from Arapree and Fibra are nearly the same, there is a reduction in strength of more than 20 % for the Fibra composite due to the braiding of the fibers.

A similar loss of tensile strength occurs to CFCC strand. The reduction of the strength from the fiber to the FRP element with the largest number of individual wires amounts to 38 %. This considerable reduction of strength has mainly two causes. One is the use of fiber prepregs. Pictures of cross-section show a variation of the fiber orientation and some air bubbles in the composite.

The second reason for the reduction of the tensile strength is the stranding of several wires of FRP to a strand. As a result of this the fiber direction deviates from the strand axis. Since carbon (and also aramid) fibers are highly orientated fibers with a very high tensile strength in the fiber axis and a low strength transverse to the fiber axis, the tensile strength of the FRP strand decreases.

The ultimate elongation of FRP is between 1,3 % and 3,8 %. Carbon fiber composites have a maximum elongation of 1,6 %, the aramid FRP range between 2,0 % and 3,7 % and the glass fiber composites range between 3,0 % and 3,8 %.

The tensile moduli are contrary to the ultimate elongation. Glass-FRP have the lowest modulus of about 70000 MPa (related to the effective fiber cross-section), aramid-FRP range between 70000 MPa and 140000 MPa, whereas carbon-FRP have moduli between 235000 MPa and 400000 MPa.

The relaxation loss of glass and carbon fiber composites is in the order of 3 % - 5 % after 100 years, whereas aramid FRP have a relaxation of 15 % - 30 %.

Stress-rupture data are only available of Arapree and Polystal. The general behaviour of carbon FRP can be deduced from tests of other applications than civil engineering. The ranking according to these tests is:

high stress-rupture strength ⟶ low stress-rupture strength
carbon FRP - aramid FRP - S-glass FRP

Fatigue tests have been carried out with aramid, carbon and glass FRP. These tests have shown, that aramid and carbon composites have a similar fatigue resistance, which is higher than that of prestressing steel, whereas the fatigue of glass FRP is considerably lower.

The relevant parameters to characterize the shear force capability are interlaminar shear strength and bond strength. Only a few data are available, which are in the same order of magnitude. The bond strength in concrete of the composites with a special surface treatment ranges between 7,2 MPa and 8,2 MPa, the ILLS between 35 MPa and 45 MPa.

7.4 Physical Properties

An important physical property is the coefficient of thermal expansion. The vallues parallel to the fiber axis are mainly determined by the fiber behaviour. In case of aramid FRP it is between $-1{,}8 \times 10^{-6}$/K and $-5{,}2 \times 10^{-6}$/K, in case of carbon FRP it is about $0{,}7 \times 10^{-6}$/K and for glass FRP $7{,}0 \times 10^{-6}$/K.

Of similar importance is the coefficient of thermal elongation transverse to the fiber axis, as damages in demonstration projects have shown. For Arapree a value of $50x10^{-6}/K$ has been measured. The coefficients of thermal elongation of the other composites have not been measured yet, but calculations on the basis of the fiber and the matrix resin behaviour (which is substantial), come to values between $30x10^{-6}/K$ and $50x10^{-6}/K$.

8. EVALUATION OF THE POTENTIALS AND SHORTCOMINGS OF FRP ELEMENTS AND THEIR PRODUCTION TECHNOLOGIES ON THE BASIS OF THE REQUIREMENTS OF TASK 1.1

8.1 Foreword

The requirements of the FRP as prestressed tensile elements are described in Task 1.1 separately for pre- and posttensioning. For the most part the same requirements are valid for pretensioning and posttensioning with and without bond. Therefore the following appraisal is split up only when the requirements are varying.

8.2 Mechanical Properties

8.2.1 Linear tensile strength

The short-term tensile strength of all FRP except the Kuraray PVA composite is higher than those of prestressing steel. In contrast to steel they show a noticeable reduction in the long-term strength. But the utilizable strength and the design strength are similar to that of prestressing steel and therefore generally sufficient. A reduction of strength due to corrosive environments is possible. This item will be dealt with in sec. 8.4.

8.2.2 Transverse compressive strength

Since steel is an isotropic material, its properties are the same in all directions. Therefore transverse loading of steel at saddles of anchorages is no problem, unless high pressures occur.

Because all FRP have a low transverse compressive strength and no plastic deformation capacity, attention has to be paid to multiaxial loading. Especially anchoring of FRP in posttensioning without bond is a problem. Solutions exist in some cases (e.g. by SICOM).

8.2.3 Young's modulus and failure strain

The lower modulus of aramid and glass FRP against steel has the advantage, that the loss of prestress due to the shrinkage and creep of the concrete is lower. The greater elongation at stressing due to the lower modulus does not really matter.

Concerning the ultimate limit states it should be kept in mind, that FRP are nearly totally elastic materials up to fracture without any plastic deformations. It has to be examined, whether the deformation capacity of FRP and especially of carbon fiber composites is sufficient and which strain limitations are required.

8.2.4 Bond strength

The FRP surface can easily be adjusted to distinct bond requirements in case of the prepreg technology. The classic pultrusion technology does not offer this possibility, but online adjustments are possible with modified processes.

8.2.5 Relaxation losses

Restrictions due to the relaxation are not required. The higher relaxation of aramid fiber composites is only of economic importance and does not limit its fields of application.

8.2.6 Fatigue strength

The fatigue strength of aramid and carbon FRP is twice as high than that of prestressing steel. Benefit can be taken from this property in dynamic loaded structures like railway sleepers.

Glass fiber composites have only 1/4 of the fatigue strength of steel, which limits its applications and efficiency in dynamic loaded structures.

8.3 Physical Properties

8.3.1 Poisson ratio

In terms of prestressing with direct bond the higher splitting forces in the anchorage zone due to the higher Poisson ratio are a real problem.

The problem has to be overcome by additional reinforcement or by other measures like compressible coatings on the FRP.

8.3.2 Coefficient of thermal expansion

One reason for the success of steel reinforced concrete is the same coefficient of thermal expansion of steel and concrete.

FRP have a different coefficient of thermal expansion, which leads in longitudinal direction to a slight change of the concrete prestress.

In case of prestressing with direct bond there may exist a problem due to the higher transverse coefficient of thermal elongation of the FRP. Additional splitting forces emerge which can crack the concrete. Therefore special measures have to be taken like additional reinforcement or compressible coatings of the FRP.

At posttensioning there is no problem regarding the transverse coefficient of thermal elongation, because the ducts can carry the additional splitting forces.

8.3.3 Thermal resistance

Aramid, carbon and glass fibers have a good thermal stability and high residual strengths at elevated temperatures, whereas the thermal stability of PVA fibers is bad.

The limiting factor in case of aramid, carbon and glass FRP is the matrix resin, because it has the lowest thermal stability and is responsible for the force transfer from the composite to the concrete. Depending on the kind of resin, the mechanical properties decrease between 89 °C and 200 °C, which is much lower than for steel.

To achieve a sufficient fire resistance period special attention should be paid to the anchorage zone.

8.4 Chemical Properties

The resistance against corrosion is the most important item, because this property is the biggest shortcoming of steel.

The carbon FRP show the best corrosion resistance, since carbon fibers are absolutely inert.

The corrosion resistance of aramid FRP has been tested in all relevant environments. The most corrosive environment is an alkaline medium. The findings in a solution of saturated $Ca(OH)_2$ + 0,4 n KOH result in a residual strength of 85 % after 100 years.

Durability tests of glass fiber composites show varying results. Polystal for example has a sufficient resistance, whereas tests in the U.S.A. with polygon composites (S 2 glass in a matrix of epoxy resin) gave discouraging results. Concrete beams prestressed with polygon FRP and immersed in the seawater splashzone for 9 months had a reduction in strength of 72 %. Further testing of glass FRP is required to get sufficient certainty.

8.5 Handling

FRP are about 5 times lighter and more flexible than steel, which makes handling much easier.

Special cautions during storage are not necessary contrary to prestressing steel. FRP should only be protected from impact loading from heavy tools or from surface injury.

8.6 Design Requirements

FRP can be applied according to the standards valid for prestressed concrete with some modifications.

An advantage can be taken from the crack width limitation, which is required to protect steel from corrosion. Since the FRP are not susceptible to corrosion, this requirement is irrelevant. Other desing requirements are already mentioned in Task 1.1.

9. SUGGESTIONS FOR MODIFICATIONS OF FRP ELEMENTS AND THEIR PRODUCTION TECHNOLOGIES

9.1 FRP Elements

Modifications of FRP are necessary with respect to their bond behaviour. Different coatings and surface structures should be developed.

A severe problem in prestressing with direct bond is the transverse coefficient of thermal elongation, which is about 5 times higher than that of concrete. Research in this field is necessary to overcome this problem. Possible solutions may be compressible coatings.

If the durability of composites is insufficient, the choice of matrix resins with a higher diffusion resistance might be a solution. Additional coatings can also work in the same way.

9.2 Production Technologies

The most important subject to get a FRP with good mechanical properties is the fiber orientation. Deviations of the fiber axis from the composite axis lead to significant reductions. This happens if the fibers are braided or if the fibers are twisted to strands.

The same attention has to be put to the fiber tension during production. At normal pultrusion the fibers are taken from the bobbin without care to equal tension in the fibers. Embedded in the matrix resin some fibers are slightly stressed and other fibers are not stressed. If these composites are prestressed during the application, the fibers get a different level of loading. The results are a lower tensile strength and a lower ultimate elongation.

The embedding of air bubbles in the FRP leads to a reduction of the diffusion resistance of corrosive media and therefore to a worse durability.

The parallel allignment of the fibers is also affected.

Sufficient curing of the composites is necessary to reach a high glass transition temperature of the resin, which equals a good thermal stability. Furthermore a well-cured resin has a higher degree of crosslinking and therefore a better diffusion resistance. If online curing is not sufficient, an additional offline curing is required.